AD NUMBER

0531 281

CLASSIFICATION CHANGES

TO

UNCLASSIFIED

FROM

SECRET

AUTHORITY

31 DEC 89, IAW OCA MRKNGS ON DOC

NRL Report 7765
Copy No. 186

Probability of Detecting Ships With an OTH Radar System

[Unclassified Title]

JON DAVID WILSON

Radar Analysis Staff
Radar Division

July 10, 1974

NAVAL RESEARCH LABORATORY
Washington, D.C.

NATIONAL SECURITY INFORMATION

Unauthorized Disclosure Subject to Criminal Sanctions.

REPORT DOCUMENTATION PAGE		READ INSTRUCTIONS BEFORE COMPLETING FORM
1. REPORT NUMBER NRL Report 7765	2. GOVT ACCESSION NO.	3. RECIPIENT'S CATALOG NUMBER
4. TITLE (and Subtitle) PROBABILITY OF DETECTING SHIPS WITH AN OTH RADAR SYSTEM [Unclassified Title]		5. TYPE OF REPORT & PERIOD COVERED This is an interim report; work is continuing 6. PERFORMING ORG. REPORT NUMBER
7. AUTHOR(s) Jon David Wilson		8. CONTRACT OR GRANT NUMBER(s)
9. PERFORMING ORGANIZATION NAME AND ADDRESS Naval Research Laboratory Washington, D.C. 20375		10. PROGRAM ELEMENT, PROJECT, TASK AREA & WORK UNIT NUMBERS R02-46A WF 12-111-704
11. CONTROLLING OFFICE NAME AND ADDRESS Department of the Navy Naval Air Systems Command Washington, D.C. 20361		12. REPORT DATE July 10, 1974 13. NUMBER OF PAGES 46
14. MONITORING AGENCY NAME & ADDRESS(if different from Controlling Office)		15. SECURITY CLASS. (of this report) SECRET 15a. DECLASSIFICATION/DOWNGRADING SCHEDULE XGDS (3) - 1989

16. DISTRIBUTION STATEMENT (of this Report)

Distribution limited to U.S. Government Agencies only; test and evaluation; July 1974. Other requests for this document must be referred to the Director, Naval Research Laboratory, Washington, D.C. 20375.

17. DISTRIBUTION STATEMENT (of the abstract entered in Block 20, if different from Report)

18. SUPPLEMENTARY NOTES

19. KEY WORDS (Continue on reverse side if necessary and identify by block number)

Over-the-horizon radar
Probability of ships detection
Probability of skywave propagation
Sea clutter spectrum

20. ABSTRACT (Continue on reverse side if necessary and identify by block number)

(U) An over-the-horizon (OTH) radar uses ionospheric reflection of high-frequency radio waves to propagate to areas far beyond the normal radar horizon. Two principle probabilities are associated with an OTH radar: the probability of successfully propagating to a given region via the ionosphere and the probability of detecting a target in sea clutter, given that propagation occurred. A particular radar system was examined and tables of probabilities were generated for various ionospheric and target parameters. An example illustrates the method of combining these probabilities to obtain a composite probability of
(Continued)

20. Abstract (Continued)

detection. The probability of propagating was calculated by a computer program that used radar parameters, the ionospheric parameters, the geographical location, and the time of day and year as inputs. The probability of detection involved a computer implementation of the radar range equation.

CONTENTS

PROBABILITY OF DETECTING SHIPS WITH AN OTH RADAR SYSTEM
[Unclassified Title]

INTRODUCTION

(U) This report is based on one phase of a study being conducted at the Naval Research Laboratory (NRL) [1-6] to compare the cost and effectiveness of three different radar systems used for ocean surveillance. The three candidate systems are an airborne radar, a satellite-borne radar, and a ground-based over-the-horizon (OTH) radar. For this report, the probability of detection of one particular OTH system has been calculated. The methods used, however, can be applied to any OTH system.

PROBABILITY OF PROPAGATION

(S) The ability of a radar system to propagate to a given range at a given time of the year was found by using RADARC, which is a computer program written by the Institute of Telecommunication Sciences to meet OTH radar analysis requirements as specified by NRL [7]. This program calculates the median clutter-to-noise ratio (C/N) for an OTH radar. The size of the backscatter area is calculated from virtual height ionograms using geometrical optics techniques. The noise considered includes atmospheric, galactic, and man-made sources. Atmospheric and ionospheric losses are included and the C/N is calculated from the radar range equation. This calculation was performed for sporadic E, E, F_1, and F_2 layer propagation modes. If the clutter return and signal return are assumed to be affected by the ionosphere in a similar manner, propagation is defined by requiring the signal return from 1000-m^2 target to be large enough against noise to yield a probability of detection P_D equal to 0.9 and a probability of false alarm P_{fa} equal to 10^{-6} for a Type 1 OTH FM-CW radar system [6]. This system has the following parameters:

100-kw average power
0.1-s frequency sweep (prf = 10 per second)
20-μs compressed pulse length
2.5-km horizontal aperture, receive ($\approx 0.25^\circ - 1^\circ$), transmit ($\approx 6^\circ - 10^\circ$).

We now calculate the C/N required for propagation.

(S) First, in order to obtain a $P_{fa} = 10^{-6}$ and a $P_D = 0.9$, the integrated signal-to-noise ration (S/N) should be 13 dB. The FM-CW radar system is assumed to have 10 frequency sweeps per second, a coherent integration time of 25 s, and a total integration time of 250 s. From Rubin and Difranco [8], the noncoherent integration gain for 10 noncoherent pulses is found to be 7 dB. With coherent integration, the noise spectrum extends from -5 to +5 Hz and is separated into 250 doppler bins of width 0.04 Hz. Thus,

Note: Manuscript submitted May 14, 1974.

the required *S/N* per doppler bin is 6 dB, (13 dB - 7 dB), and the *S/N* in a cycle bandwidth is -8 dB, or [6 dB + 10 log (0.04)]. Since the signal and clutter are assumed to propagate in a similar manner, the signal-to-clutter ratio (*S/C*) is given by

$$\frac{S}{C} = \frac{\sigma_T}{\frac{\sigma_0 \theta_B R c \tau}{2}} = -33 \text{ dB} \qquad (1)$$

where

σ_T = target cross section (30 dBsm),

σ_0 = relative sea clutter cross section (-17 dB)

θ_B = antenna beamwidth (1°)

R = radar range, 1000 n.mi.

c = speed of light

τ = effective pulse width, 20 μs.

Now, the required *C/N* for propagation is calculated from

$$\frac{C}{N} = \frac{\frac{S}{N}}{\frac{S}{C}} = 25 \text{ dB.*} \qquad (2)$$

Even though the madre antenna pattern is wired into RADARC, the received clutter and noise powers are independent of the receive antenna beamwidth,† and consequently, RADARC can be used to calculate propagation for the FM-CW radar system. The only alterations made to the program were to eliminate printed output and to add the punched output used in calculating the propagation statistics.

(S) The ability to propagate was found for four months, (January, April, July, or October), two times (day or night), and three sunspot numbers (20, 45, or 75, which are the 25th, 50th, and 75th percentiles). The radar is situated in Maine (latitude 45° N, longitude 67° W). For each of the 24 conditions, the radar model RADARC was used to calculate the *C/N* every 2 hr for three azimuth angles (14°, 59°, and 104°), spanning a 90° sector. For each set of parameters, one-bounce propagation via four layers (sporadic *E*, *E*, F_1, F_2) was considered and the maximum *C/N* chosen. The number of occasions out of 18 (6 times, 2 hr apart, and 3 azimuths) that the *C/N* exceeded 25 dB is given in Tables 1-24. We can interpret these numbers divided by 18 as a probability of propagation. If

*Specifically, a *C/N* of 25 dB is equivalent to our defined propagation at 1000 n.mi. for a 30-dB target and the particular frequency that yields a 1° beamwidth. For other ranges, targets, and frequencies, 25 dB was still used since *C/N* varies rapidly with range and hence a change in the threshold (25 dB) would have little effect on the region of propagation.

†When the transmit beamwidth is larger than the receive beamwidth, the receive array is sampling an extended source. When the beamwidth narrows, the clutter (or atmospheric noise) patch narrows, but the gain of the array increases.

(U) Table 1
Number of successful propagations out of 18 possible opportunities, in January, in nighttime with SNS=20 as a function of range and frequency

MONTH = JAN NIGHT SUN SPOT = 20

RANGE (NM)	FREQUENCY (MHZ) 6	9	12	15	18	21	24	27
500	16	13	9	0	0	0	0	0
1000	18	16	13	10	7	3	0	0
1500	17	2	0	0	0	0	0	0
2000	15	5	0	0	0	0	0	0

(U) Table 2
Number of successful propagations out of 18 possible opportunities, in January, in daytime with SSN=20 as a function of range and frequency

MONTH = JAN DAY SUN SPOT = 20

RANGE (NM)	FREQUENCY (MHZ) 6	9	12	15	18	21	24	27
500	18	18	9	0	0	0	0	0
1000	16	18	18	14	4	0	0	0
1500	3	9	13	12	8	3	0	0
2000	2	4	4	5	5	5	0	0

(U) Table 3
Number of successful propagations out of 18 possible opportunities, in April, in nighttime with SSN=20 as a function of range and frequency

MONTH = APR NIGHT SUN SPOT = 20

RANGE (NM)	FREQUENCY (MHZ) 6	9	12	15	18	21	24	27
500	18	12	6	0	0	0	0	0
1000	18	16	12	8	3	0	0	0
1500	15	8	4	0	0	0	0	0
2000	12	10	5	1	0	0	0	0

(U) Table 4
Number of successful propagations out of 18 possible opportunities, in April, in daytime with SSN=20 as a function of range and frequency

MONTH = APR DAY SUN SPOT = 20

RANGE (NM)	FREQUENCY (MHZ) 6	9	12	15	18	21	24	27
500	18	18	4	0	0	0	0	0
1000	8	16	15	11	2	0	0	0
1500	0	4	9	10	1	0	0	0
2000	0	2	5	7	5	0	0	0

(U) Table 5
Number of successful propagations out of 18 possible opportunities, in July, in nighttime with SSN=20 as a function of range and frequency

MONTH = JUL NIGHT SUN SPOT = 20

RANGE (NM)	FREQUENCY (MHZ) 6	9	12	15	18	21	24	27
500	18	18	15	4	3	0	0	0
1000	18	18	18	17	15	8	5	2
1500	13	11	6	1	0	0	0	0
2000	7	11	6	3	0	0	0	0

(U) Table 6
Number of successful propagations out of 18 possible opportunities, in July, in daytime with SSN=20 as a function of range and frequency

MONTH = JUL DAY SUN SPOT = 20

RANGE (NM)	FREQUENCY (MHZ) 6	9	12	15	18	21	24	27
500	17	16	16	2	1	0	0	0
1000	5	13	17	10	13	13	6	1
1500	0	3	9	8	0	0	0	0
2000	0	1	2	3	3	0	0	0

(U) Table 7
Number of successful propagations out of 18 possible opportunities, in October, in nighttime with SSN=20 as a function of range and frequency

MONTH = OCT NIGHT SUN SPOT = 20

	FREQUENCY (MHZ)							
RANGE (NM)	6	9	12	15	18	21	24	27
500	18	15	9	2	0	0	0	0
1000	18	18	15	12	8	4	2	0
1500	16	7	1	0	0	0	0	0
2000	14	10	1	0	0	0	0	0

(U) Table 8
Number of successful propagations out of 18 possible opportunities, in October, in daytime with SSN=20 as a function of range and frequency

MONTH = OCT DAY SUN SPOT = 20

	FREQUENCY (MHZ)							
RANGE (NM)	6	9	12	15	18	21	24	27
500	18	18	9	0	0	0	0	0
1000	11	18	18	17	6	2	0	0
1500	3	7	14	15	8	2	0	0
2000	0	4	6	9	13	7	0	0

(U) Table 9
Number of successful propagations out of 18 possible opportunities, in January, in nighttime with SSN=45 as a function of range and frequency

MONTH = JAN NIGHT SUN SPOT = 45

RANGE (NM)	FREQUENCY (MHZ) 6	9	12	15	18	21	24	27
500	16	13	8	0	0	0	0	0
1000	18	16	13	9	5	3	0	0
1500	17	5	0	0	0	0	0	0
2000	15	11	0	0	0	0	0	0

(U) Table 10
Number of successful propagations out of 18 possible opportunities, in January, in daytime with SSN=45 as a function of range and frequency

MONTH = JAN DAY SUN SPOT = 45

RANGE (NM)	FREQUENCY (MHZ) 6	9	12	15	18	21	24	27
500	18	18	13	0	0	0	0	0
1000	15	18	18	16	7	0	0	0
1500	3	8	15	14	11	7	2	0
2000	1	6	9	5	8	7	5	0

(U) Table 11
Number of successful propagations out of 18 possible opportunities, in April, in nighttime with SSN=45 as a function of range and frequency

MONTH = APR NIGHT SUN SPOT = 45

RANGE (NM)	FREQUENCY (MHZ) 6	9	12	15	18	21	24	27
500	18	13	5	0	0	0	0	0
1000	18	17	14	8	3	0	0	0
1500	14	14	5	2	0	0	0	0
2000	12	13	8	4	0	0	0	0

(U) Table 12
Number of successful propagations out of 18 possible opportunities, in April, in daytime with SSN=45 as a function of range and frequency

MONTH = APR DAY SUN SPOT = 45

RANGE (NM)	FREQUENCY (MHZ) 6	9	12	15	18	21	24	27
500	17	18	3	0	0	0	0	0
1000	5	13	18	9	2	0	0	0
1500	0	3	8	12	7	0	0	0
2000	0	2	5	6	8	4	0	0

(U) Table 13
Number of successful propagations out of 18 possible opportunities, in July, in nighttime with SSN=45 as a function of range and frequency

MONTH = JUL NIGHT SUN SPOT = 45

RANGE (NM)	FREQUENCY (MHZ) 6	9	12	15	18	21	24	27
500	18	18	15	3	2	0	0	0
1000	18	18	18	16	14	8	5	2
1500	12	15	7	3	0	0	0	0
2000	6	14	6	6	1	0	0	0

(U) Table 14
Number of successful propagations out of 18 possible opportunities, in July, in daytime with SSN=45 as a function of range and frequency

MONTH = JUL DAY SUN SPOT = 45

RANGE (NM)	FREQUENCY (MHZ) 6	9	12	15	18	21	24	27
500	16	18	15	2	1	0	0	0
1000	5	11	17	8	13	13	6	1
1500	0	2	6	13	1	0	0	0
2000	0	0	2	2	8	0	0	0

(U) Table 15
Number of successful propagations out of 18 possible opportunities, in October, in nighttime with SSN=45 as a function of range and frequency

MONTH = OCT NIGHT SUN SPOT = 45

RANGE (NM)	FREQUENCY (MHZ) 6	9	12	15	18	21	24	27
500	18	15	9	0	0	0	0	0
1000	18	18	15	12	8	4	1	0
1500	15	12	3	0	0	0	0	0
2000	14	14	5	1	0	0	0	0

(U) Table 16
Number of successful propagations out of 18 possible opportunities, in October, in daytime with SSN=45 as a function of range and frequency

MONTH = OCT DAY SUN SPOT = 45

RANGE (NM)	FREQUENCY (MHZ) 6	9	12	15	18	21	24	27
500	18	18	16	0	0	0	0	0
1000	10	13	18	17	13	1	0	0
1500	3	6	12	18	14	8	2	0
2000	0	2	5	9	13	13	8	1

(U) Table 17
Number of successful propagations out of 18 possible opportunities, in January, in nighttime with SSN=75 as a function of range and frequency

MONTH = JAN NIGHT SUN SPOT = 75

RANGE (NM)	FREQUENCY (MHZ) 6	9	12	15	18	21	24	27
500	16	13	8	0	0	0	0	0
1000	18	15	13	9	4	1	0	0
1500	18	10	1	0	0	0	0	0
2000	15	14	2	0	0	0	0	0

(U) Table 18
Number of successful propagations out of 18 possible opportunities, in January, in daytime with SSN=75 as a function of range and frequency

MONTH = JAN DAY SUN SPOT = 75

RANGE (NM)	FREQUENCY (MHZ) 6	9	12	15	18	21	24	27
500	18	18	12	2	0	0	0	0
1000	2	18	18	16	9	4	0	0
1500	3	7	13	16	13	10	5	2
2000	2	4	7	12	10	10	7	5

(U) Table 19
Number of successful propagations out of 18 possible opportunities, in April, in nighttime with SSN=75 as a function of range and frequency

MONTH = APR NIGHT SUN SPOT = 75

RANGE (NM)	FREQUENCY (MHZ) 6	9	12	15	18	21	24	27
500	18	14	5	0	0	0	0	0
1000	18	18	14	8	3	0	0	0
1500	15	18	11	4	0	0	0	0
2000	11	15	14	6	2	0	0	0

(U) Table 20
Number of successful propagations out of 18 possible opportunities, in April, in daytime with SSN=75 as a function of range and frequency

MONTH = APR DAY SUN SPOT = 75

RANGE (NM)	FREQUENCY (MHZ) 6	9	12	15	18	21	24	27
500	16	18	7	0	0	0	0	0
1000	5	14	18	14	4	0	0	0
1500	0	3	7	12	11	5	0	0
2000	0	2	4	7	11	10	3	0

(U) Table 21
Number of successful propagations out of 18 possible opportunities, in July, in nighttime with SSN=75 as a function of range and frequency

MONTH = JUL NIGHT SUN SPOT = 75

RANGE (NM)	FREQUENCY (MHZ) 6	9	12	15	18	21	24	27
500	18	18	14	3	1	0	0	0
1000	18	18	18	15	14	7	5	1
1500	12	15	10	6	1	0	0	0
2000	6	14	13	7	4	0	0	0

(U) Table 22
Number of successful propagations out of 18 possible opportunities, in July, in daytime with SSN=75 as a function of range and frequency

MONTH = JUL DAY SUN SPOT = 75

RANGE (NM)	FREQUENCY (MHZ) 6	9	12	15	18	21	24	27
500	14	18	17	1	1	0	0	0
1000	2	10	18	9	17	16	5	1
1500	0	2	5	13	4	0	0	0
2000	0	0	2	3	7	1	0	0

(U) Table 23
Number of successful propagations out of 18 possible opportunities, in October, in nighttime with SSN=75 as a function of range and frequency

MONTH = OCT NIGHT SUN SPOT = 75

	FREQUENCY (MHZ)							
RANGE (NM)	6	9	12	15	18	21	24	27
500	18	15	9	0	0	0	0	0
1000	18	18	15	12	7	3	0	0
1500	15	15	7	1	0	0	0	0
2000	13	17	12	3	0	0	0	0

(U) Table 24
Number of successful propagations out of 18 possible opportunities, in October, in daytime with SSN=75 as a function of range and frequency

MONTH = OCT DAY SUN SPOT = 75

	FREQUENCY (MHZ)							
RANGE (NM)	6	9	12	15	18	21	24	27
500	18	18	17	4	0	0	0	0
1000	9	18	18	18	16	7	0	0
1500	2	5	11	18	15	14	8	3
2000	0	3	6	9	16	13	13	8

the tables are compared, the following general conclusions can be reached about propagation when using the optimal frequency for a given range:

- Better at night than during the day
- Better in winter than in summer
- For the sunspot numbers considered, better for the higher sunspot numbers
- Propagation is very close to 100% for the shorter ranges.

The following conclusions can be reached about frequency preferences:

- Higher frequencies during daytime
- Higher frequencies during summertime
- Higher frequencies for higher sunspot numbers
- Higher frequencies for longer ranges.

PROBABILITY OF DETECTION

(U) In the previous section successful propagation was defined in terms of detection of targets against noise. Consequently, in this section we will consider only the detection of targets in sea clutter.

(C) The basic assumption is that the target return (small region) and the clutter return (extended region) will be affected in the same way by passage through the ionosphere. This allows us to calculate the *S/C* at the input to the processor from the target and clutter radar cross sections. The principal signal enhancement is from doppler processing with an additional noncoherent integration of the doppler cells.

(S) The *S/C* was calculated from Eq. (1) with three different target cross sections, 1000-m^2 and 3000-m^2 destroyers and a 50,000-m^2 aircraft carrier; and four ranges, 500, 1000, 1500, and 2000 n.mi, for each target type. The doppler processing gain was calculated for a set of radial velocities from -30 to +30 knots and a range of operating frequencies from 5 to 30 MHz. We assumed the target to be in one doppler cell and a 2-dB loss for processing and target doppler spread. The clutter level in a given doppler cell was obtained by normalizing a sample clutter spectrum. Two sample clutter spectra were derived from a working paper by Dr. James R. Barnum of Standford Research Institute [9]. One asymmetrical spectrum represents the type of clutter spectrum observed with approaching (or receding) winds. The other spectrum is symmetric and is typical of the spectra observed in crosswind conditions.

(U) One observed clutter spectrum was used to generate both spectra. This particular spectrum was chosen on the basis of its clean appearance, but all of the candidate spectra from Ref. 9 have certain features in common, such as the Bragg scatter peaks, the lowered level of clutter between these peaks, and the even lower level of clutter in the doppler cells outside of the peak. The symmetrical (crosswind) clutter spectrum was obtained by averaging the clutter cells symmetrically placed about the carrier frequency. This process yielded a spectrum that appears to be a valid approximation to observed

crosswind spectra. This approximation was used because there was always at least a small asymmetry in the levels of the approaching and receding Bragg scattering lines of the observed spectra (an asymmetry would favor either the approaching or receding targets).

(U) The asymmetrical clutter spectrum is shown in Fig. 1. This spectrum was extended to ±5 Hz at a -42 dB level. The sea clutter, of course, does not have a plateau at some particular level below the Bragg line peak but has been measured on the Madre radar (with a 70-dB dynamic range) to drop off to at least 65 to 70 dB below the peak at ±5 Hz. The -42 dB plateau seems to be a feature of the radar on which the spectrum was measured. This would make little difference in our results: If the target is not in a Bragg line peak, it is detected. The two large spikes correspond to the Bragg scatter of ocean waves. The relative amplitude of the two spikes is a function of the angle of the ocean wavefront to the radar wavefront and hence depends on local wind direction [10]. The doppler offset of these spikes from the carrier frequency depends on the carrier frequency. The particular spectrum shown as measured at 20 MHz. At other radar frequencies, the spectral line spacing expands and contracts with the square root of the carrier frequency [11].

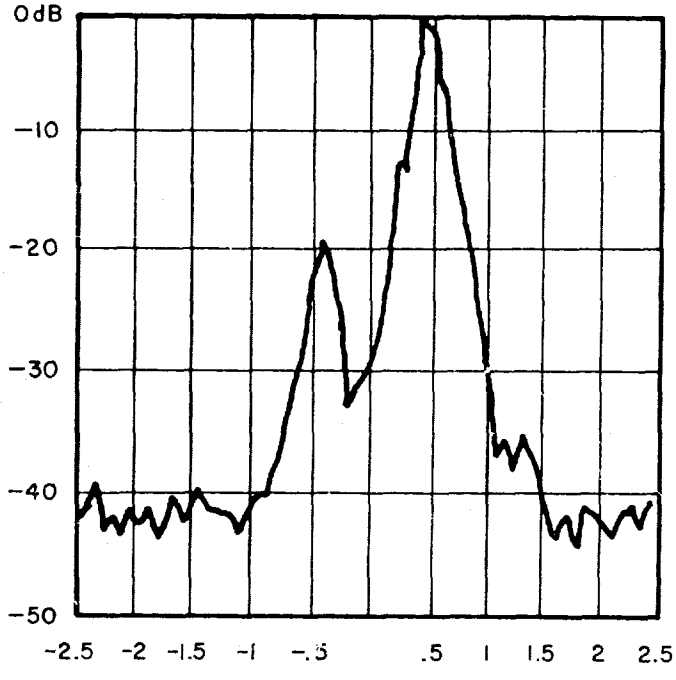

(U) Fig. 1—Typical clutter doppler spectrum

(S) The doppler cell in which the target appears is calculated from the radial speed V_r and operating wavelength λ by

$$\text{Doppler cell} = \frac{2V_r}{\lambda(0.04)}. \tag{3}$$

(S) The clutter energy in that cell is calculated from the normalized clutter spectrum (shifted by the operating frequency). The *S/C* obtained for this radial speed and operating frequency combination is interpolated into a table of values, giving the P_d for 10 pulses [8]. For purposes of display, an array of symbols indicating the probability level for each combination of speed and frequency is printed. The P_d results for the approaching wind clutter spectrum are given in Figs. 2-13 and the crosswind results are given in Figs. 14-25. In the figures, an integer N indicates that P_d is between $0.1(N)$ and $0.1(N + 1)$ and a blank indicates that P_d is less than 0.1. The following observations can be made.

- Smaller targets can be detected only at the higher radial velocities, whereas the largest target can be detected in all doppler cells except those occupied by the Bragg scatter lines.

- Better detection performance is observed in the nonsymmetrical spectrum. This can be attributed (a) to the concentration of clutter energy in the larger Bragg scatter peak where detection is impossible in any case, and (b) to the consequent reduction of clutter energy in the remaining doppler cells.

- Targets can be detected in more of the doppler cells at higher frequencies. This is because the target doppler is proportional to frequency, whereas the clutter spectrum expands as the square root of the frequency. Thus, as the frequency is raised targets obscured by the clutter peak move into doppler cells of lower clutter.

(U) This last point may be the result of using one clutter spectrum taken at one carrier frequency and expanded and contracted for other frequencies. The clutter spectrum is affected by both sea state and frequency, but we did not have available sufficient data to make quantitative adjustment to the assumed spectrum. The doppler level in the cells away from the Bragg lines increases with the carrier frequency, and our sample spectrum was measured at a relatively high frequency. This means that at low frequencies the clutter levels used in our calculation are too high, but again, it would not affect our results; if a target is not in a Bragg line peak, it is detected.

(U) The preceding detection curves (Figs. 2-25) were based on the assumption that $\sigma_0 = -17$ dB. However, since there is some controversy over the value of σ_0 (Barnum has data that indicate $\sigma_0 = -23$ dB [12]), additional detection curves are generated for $\sigma_0 = -23$ dB. These curves are displayed in Figs. 26-49. Obviously the only difference between the results and the previous results is an improvement of 6 dB.

RESULTS

(S) To obtain a composite P_d, we multiply the probability of propagation (from Tables 1-24) by the probability of detection given that propagation is successful (Figs. 2-49). Two examples, one for $\sigma_0 = -17$ dB the other for $\sigma_0 = -23$ dB, are shown in Figs. 50 and 51, respectively. The composite P_d for each of four ranges is plotted vs radial speed. The target has a 3000-m^2 radar cross section in April, in daytime under crosswind conditions, with a sunspot number of 45. The operating frequency for each range is the frequency that yields the best composite P_d over the largest speed range. Only closing speeds are shown because of the symmetrical clutter spectrum. From these curves it appears that it is very difficult to detect a 3000-m^2 target at radial speeds below 15 knots if $\sigma_0 = -17$ dB and

RADIAL SPEED (KNOTS)

	-30	-25	-20	-15	-10	-5	0	5	10	15	20	25	30
5	999999999961					13321							3
6	99999999999982					25421							1599
7	999999999999994					137542							279999
8	9999999999999961					158753							38999999
9	999999999999999971					29865							599999999
10	9999999999999999982					379761							16999999999
11	9999999999999999993					1489871							179999999999
12	99999999999999999994					599982							28999999999999
13	99999999999999999995					299982							38999999999999
14	999999999999999999991					399993							49999999999999
15	999999999999999999996					499994							599999999999999
16	9999999999999999999971					48999							1999999999999999
17	999999999999999999992					59999							6999999999999999
18	999999999999999999998					199991							17999999999999999
19	999999999999999999999					199991							29999999999999999
20	9999999999999999999994					299991							89999999999999999
21	9999999999999999999994					299991							399999999999999999
22	9999999999999999999995					399992							399999999999999999
23	9999999999999999999999					389992							999999999999999999
24	99999999999999999999991					99993							4999999999999999999
25	99999999999999999999991					99993							5999999999999999999
26	99999999999999999999996					99993							15999999999999999999
27	99999999999999999999997					99994							19999999999999999999
28	99999999999999999999997					199994							19999999999999999999
29	99999999999999999999998					199995							69999999999999999999
30	999999999999999999999992					199995							79999999999999999999

(S) Fig. 2—P_d of 1000 m^2 target at 500-n.mi. range in approaching sea clutter, σ_0 = -17 dB

RADIAL SPEED (KNOTS)

	-30	-25	-20	-15	-10	-5	0	5	10	15	20	25	30
5	9999999994												
6	9999999999961												27
7	99999999999982												4999
8	999999999999994					1							1699999
9	9999999999999995					21							29999999
10	99999999999999961					121							899999999
11	999999999999999997					1411							19999999999
12	9999999999999999982					2521							199999999999
13	9999999999999999999					3631							1699999999999
14	99999999999999999994					4742							7999999999999
15	99999999999999999995					4743							39999999999999
16	999999999999999999991					1873							3899999999999999
17	999999999999999999996					2974							4999999999999999
18	9999999999999999999971					2985							9999999999999999
19	999999999999999999999992					3985							59999999999999999
20	999999999999999999999992					3996							19999999999999999999
21	999999999999999999999998					4896							69999999999999999999
22	999999999999999999999999					4897							79999999999999999999
23	9999999999999999999999994					1997							299999999999999999999
24	99999999999999999999999994					2998							299999999999999999999
25	99999999999999999999999995					2998							899999999999999999999
26	99999999999999999999999999					2999							999999999999999999999
27	999999999999999999999999991					3999							4999999999999999999999
28	999999999999999999999999991					3999							4999999999999999999999
29	999999999999999999999999991					3999							9999999999999999999999
30	9999999999999999999999999996					4999							9999999999999999999999

(S) Fig. 3 - P_d of 1000-m^2 target at 1000-n.mi. range in approaching sea clutter, σ_0 = -17 dB

RADIAL SPEED (KNOTS)

	-30	-25	-20	-15	-10	-5	0	5	10	15	20	25	30
5	9999999751												
6	999999999972												3
7	9999999999983												1567
8	99999999999995												168998
9	999999999999961												7999999
10	9999999999999972												489999999
11	99999999999999983						1						5999999999
12	99999999999999994						1						69999999999
13	999999999999999995						2						299999999999
14	9999999999999999951						2						2799999999999
15	9999999999999999991						131						8999999999999
16	9999999999999999997						42						49999999999999
17	99999999999999999972						531						199999999999999
18	99999999999999999992						541						599999999999999
19	99999999999999999998						641						1999999999999999
20	99999999999999999999						652						6999999999999999
21	999999999999999999994						1452						27999999999999999
22	999999999999999999995						1463						39999999999999999
23	999999999999999999999						563						89999999999999999
24	9999999999999999999991						574						89999999999999999
25	9999999999999999999991						574						499999999999999999
26	9999999999999999999996						674						499999999999999999
27	9999999999999999999997						685						999999999999999999
28	9999999999999999999997						785						199999999999999999
29	9999999999999999999999						796						699999999999999999
30	99999999999999999999992						1796						699999999999999999

(S) Fig. 4—P_d of 1000-m^2 target at 1500-n.mi. range in approaching sea clutter, σ_0 = -17 dB

RADIAL SPEED (KNOTS)

	-30	-25	-20	-15	-10	-5	0	5	10	15	20	25	30
5	999986642												
6	99999999863												1
7	9999999999751												234
8	99999999999992												35675
9	999999999999993												4678867
10	9999999999999994												157897689
11	99999999999999951												2689987999
12	99999999999999991												27999999999
13	99999999999999999972												89999999999
14	99999999999999999992						1						149999999999
15	99999999999999999998						1						59999999999999
16	999999999999999999994						1						19999999999999
17	999999999999999999994						21						699999999999999
18	999999999999999999991						21						299999999999999
19	999999999999999999996						31						799999999999999
20	999999999999999999996						32						3899999999999999
21	999999999999999999999991						12						4999999999999999
22	999999999999999999999992						131						19999999999999999
23	999999999999999999999998						231						59999999999999999
24	999999999999999999999998						241						59999999999999999
25	999999999999999999999998						241						199999999999999999
26	999999999999999999999993						352						299999999999999999
27	999999999999999999999994						352						699999999999999999
28	999999999999999999999994						452						799999999999999999
29	999999999999999999999998						462						2999999999999999999
30	999999999999999999999998						463						3999999999999999999

(S) Fig. 5—P_d of 1000-m^2 target at 2000-n.mi. range in approaching sea clutter, σ_0 = -17 dB

RADIAL SPEED (KNOTS)

	-30	-25	-20	-15	-10	-5	0	5	10	15	20	25	30
5	999999999999661					489999994						599	
6	99999999999982					1699999961						1179999	
7	9999999999999994					2799999971						38999999	
8	99999999999999961					499999993						4999999999	
9	999999999999999971					599999994						159999999999	
10	9999999999999999992					1699999995						17999999999999	
11	99999999999999999993					299999991						27999999999999	
12	999999999999999999941					289999991						89999999999999	
13	999999999999999999991					399999992						499999999999999	
14	9999999999999999999961					99999992						5999999999999999	
15	9999999999999999999962					99999993						15999999999999999	
16	99999999999999999999951					169999994						19999999999999999	
17	99999999999999999999982					169999994						27999999999999999	
18	99999999999999999999982					179999995						29999999999999999	
19	99999999999999999999951					79999996						89999999999999999	
20	99999999999999999999962					29999996						48999999999999999	
21	99999999999999999999964					39999991						49999999999999999	
22	99999999999999999999995					39999991						19999999999999999	
23	99999999999999999999995					49999991						19999999999999999	
24	99999999999999999999964					49999991						69999999999999999	
25	99999999999999999999998					49999992						69999999999999999	
26	99999999999999999999998					49999992						29999999999999999	
27	99999999999999999999995					59999992						29999999999999999	
28	99999999999999999999995					59999993						29999999999999999	
29	99999999999999999999996					69999993						89999999999999999	
30	99999999999999999999998					89999993						89999999999999999	

(S) Fig. 6--P_d of 3000-m^2 target at 500-n.mi. range in approaching sea clutter, σ_0 = -17 dB

RADIAL SPEED (KNOTS)

	-30	-25	-20	-15	-10	-5	0	5	10	15	20	25	30
5	999999999995					1477643						37	
6	9999999999971					269865						5999	
7	999999999999983					1489861						1699999	
8	99999999999999994					5999982						289999999	
9	999999999999999951					3799993						4999999999	
10	99999999999999999996					4899994						59999999999	
11	999999999999999999972					5999995						1699999999999	
12	99999999999999999998					1999996						17999999999999	
13	99999999999999999999993					2799997						79999999999999	
14	99999999999999999999994					2799997						3899999999999999	
15	99999999999999999999999					3899998						9999999999999999	
16	99999999999999999999996					999993						4999999999999999	
17	999999999999999999999961					999993						9999999999999999	
18	999999999999999999999991					1599994						59999999999999999	
19	999999999999999999999992					1699994						169999999999999999	
20	999999999999999999999998					699995						199999999999999999	
21	999999999999999999999998					799996						799999999999999999	
22	999999999999999999999993					799996						2899999999999999999	
23	999999999999999999999994					899996						2999999999999999999	
24	999999999999999999999994					299997						8999999999999999999	
25	999999999999999999999951					399997						9999999999999999999	
26	999999999999999999999991					399998						4999999999999999999	
27	999999999999999999999992					499998						4999999999999999999	
28	999999999999999999999992					499998						5999999999999999999	
29	999999999999999999999992					599999						1999999999999999999	
30	999999999999999999999996					1599999						1999999999999999999	

(S) Fig. 7--P_d of 3000-m^2 target at 1000-n.mi. range in approaching sea clutter, σ_0 = -17 dB

RADIAL SPEED(KNOTS)

	-30	-25	-20	-15	-10	-5	0	5	10	15	20	25	30
5	999999999961					13321							3
6	99999999999982					25421							1599
7	999999999999994					147542							279999
8	9999999999999981					158754							48999999
9	99999999999999971					29865							599999999
10	999999999999999982					1379761							10999999999
11	999999999999999993					1489871							279999999999
12	9999999999999999994					599982							2899999999999
13	99999999999999999995					299992							39999999999999
14	999999999999999999991					399993							49999999999999
15	999999999999999999997					499994							599999999999999
16	9999999999999999999971					58999							1999999999999999
17	9999999999999999999992					59999							6999999999999999
18	99999999999999999999998					199991							17999999999999999
19	99999999999999999999999					199991							29999999999999999
20	999999999999999999999994					299991							89999999999999999
21	999999999999999999999994					299991							39999999999999999
22	999999999999999999999995					399992							39999999999999999
23	999999999999999999999999					389992							99999999999999999
24	9999999999999999999999991					99993							49999999999999999999
25	9999999999999999999999991					99993							59999999999999999999
26	9999999999999999999999997					99994							15999999999999999999
27	9999999999999999999999997					199994							19999999999999999999
28	9999999999999999999999997					199994							19999999999999999999
29	9999999999999999999999998					199995							69999999999999999999
30	99999999999999999999999992					199995							79999999999999999999

(S) Fig. 8—P_d of 3000-m^2 target at 1500-n.mi range in approaching sea clutter, σ_0 = -17 dB

RADIAL SPEED(KNOTS)

	-30	-25	-20	-15	-10	-5	0	5	10	15	20	25	30
5	99999999983					11							1
6	999999999951					21							279
7	999999999999971					1421							48999
8	9999999999999983					25421							15999999
9	99999999999999994					6532							269999999
10	999999999999999995					14653							3999999999
11	9999999999999999991					25854							49999999999
12	9999999999999999971					26965							599999999999
13	9999999999999999992					7976							16999999999999
14	9999999999999999998					189861							19999999999999
15	99999999999999999994					199971							279999999999999
16	99999999999999999994					25998							899999999999999
17	99999999999999999999					26998							3899999999999999
18	999999999999999999999995					7999							4999999999999999
19	999999999999999999999996					7999							9999999999999999
20	999999999999999999999971					8999							59999999999999999
21	999999999999999999999991					8999							199999999999999999
22	999999999999999999999992					19999							199999999999999999
23	999999999999999999999998					15999							699999999999999999
24	999999999999999999999998					69991							179999999999999999
25	999999999999999999999999					69991							299999999999999999
26	9999999999999999999999993					79991							299999999999999999
27	9999999999999999999999994					79991							399999999999999999
28	9999999999999999999999994					79991							899999999999999999
29	9999999999999999999999995					89992							3999999999999999999
30	9999999999999999999999999					89992							4999999999999999999

(S) Fig. 9—P_d of 3000-m^2 target at 2000-n.mi. range in approaching sea clutter, σ_0 = -17 dB

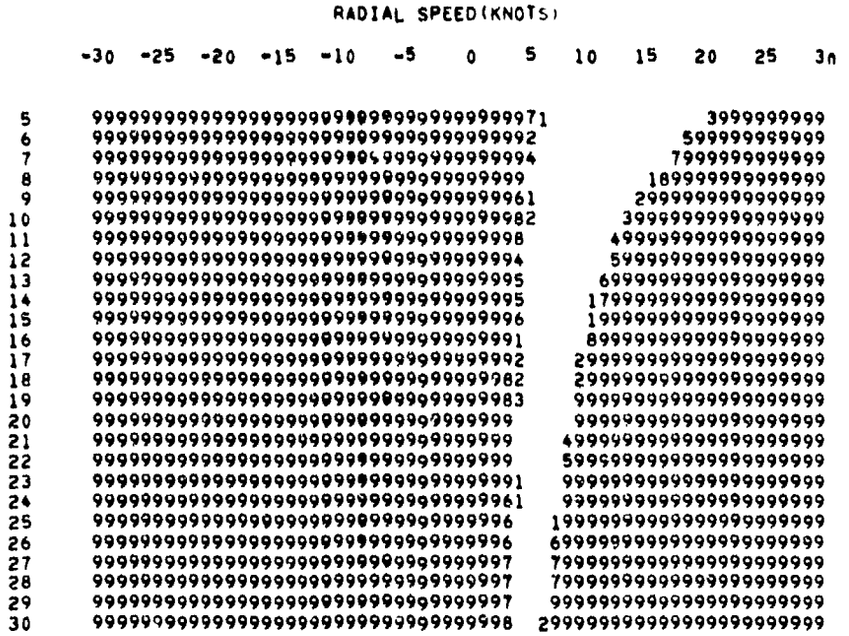

(S) Fig. 10—P_d of 50,000-m^2 target at 500-n.mi. range in approaching sea clutter, σ_0 = -17 dB

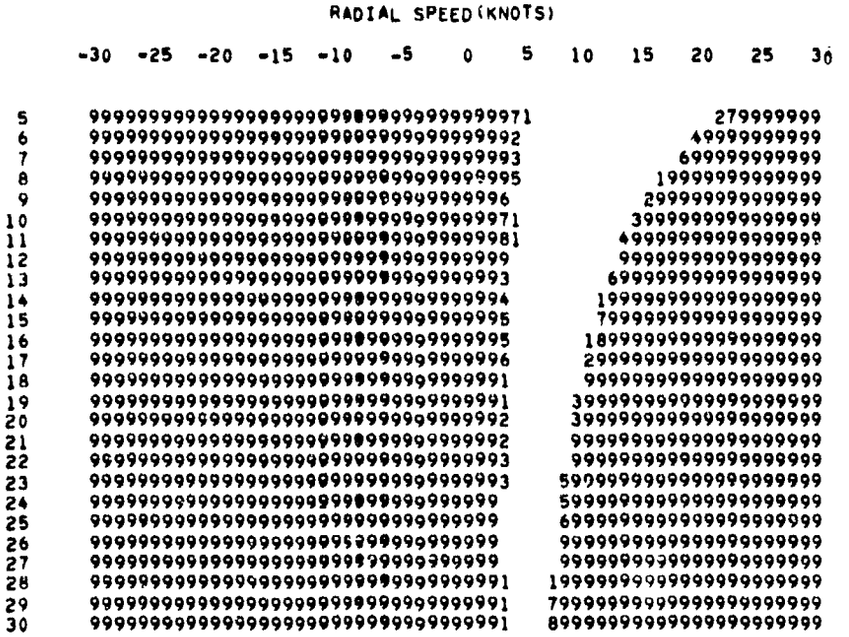

(S) Fig. 11—P_d of 50,000-m^2 target at 1000-n.mi. range in approaching sea clutter, σ_0 = -17 dB

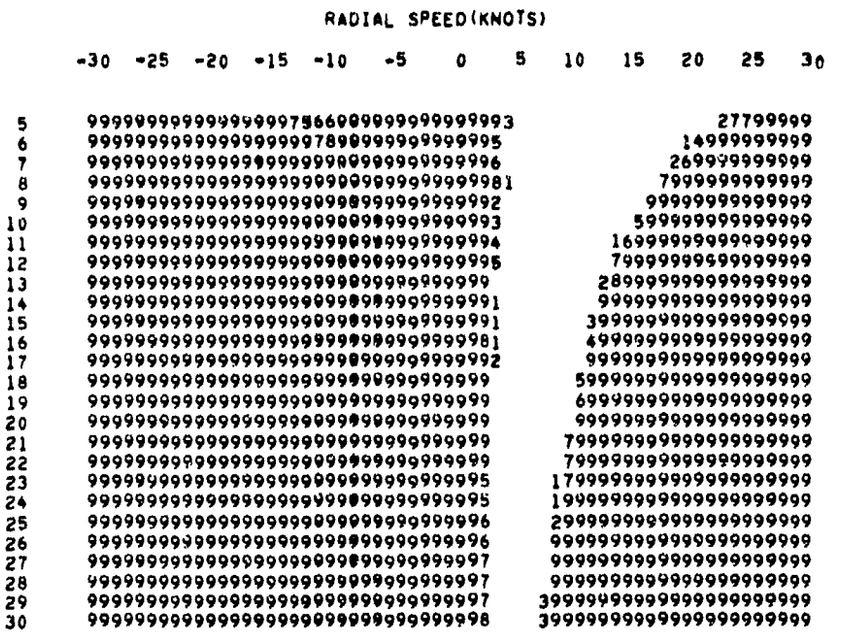

(S) Fig. 12—P_d of 50,000-m^2 target at 1500-n.mi. range in approaching sea clutter, σ_0 = −17 dB

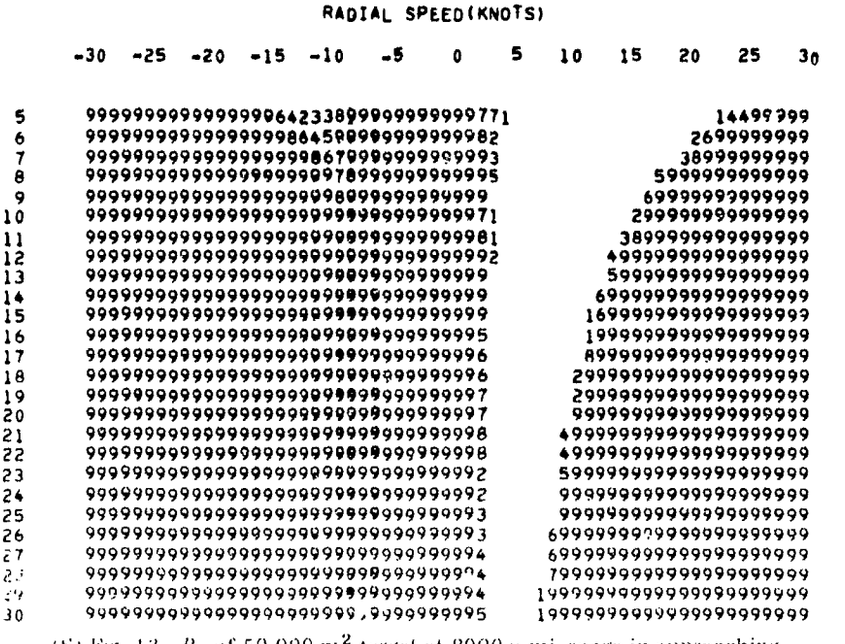

(S) Fig. 13—P_d of 50,000-m^2 target at 2000 n.mi. range in approaching sea clutter, σ_0 = −17 dB

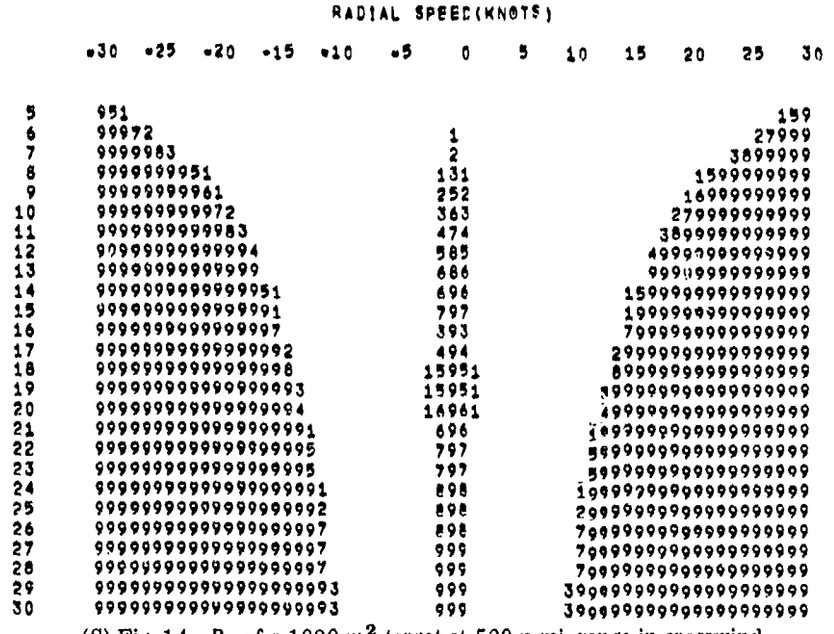

(S) Fig. 14—P_d of a 1000-m^2 target at 500-n.mi. range in crosswind sea clutter, σ_0 = -17 dB

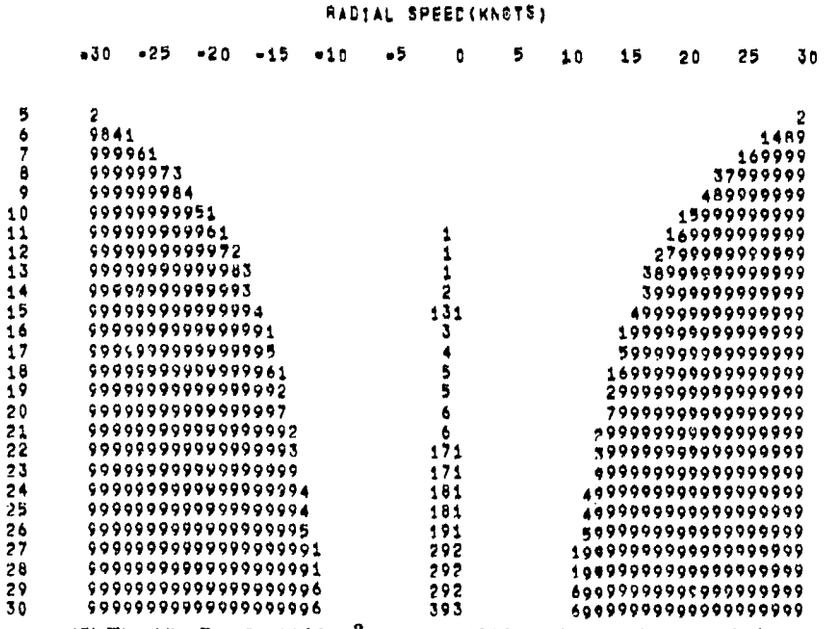

(S) Fig. 15—P_d of a 1000-m^2 target at 1000-n.mi. range in crosswind sea clutter, σ_0 = -17 dB

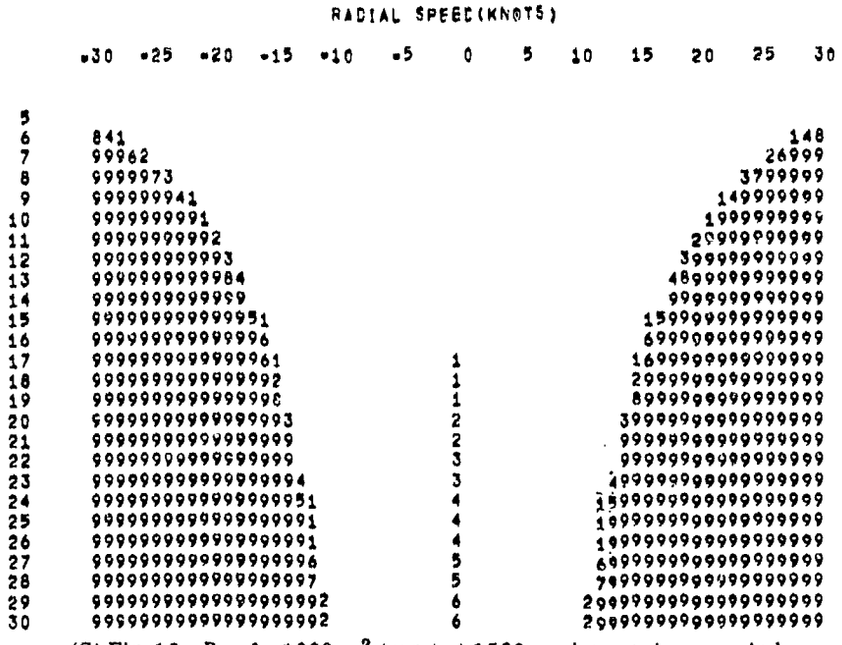

(S) Fig. 16—P_d of a 1000-m^2 target at 1500-n.mi. range in crosswind sea clutter, σ_0 = -17 dB

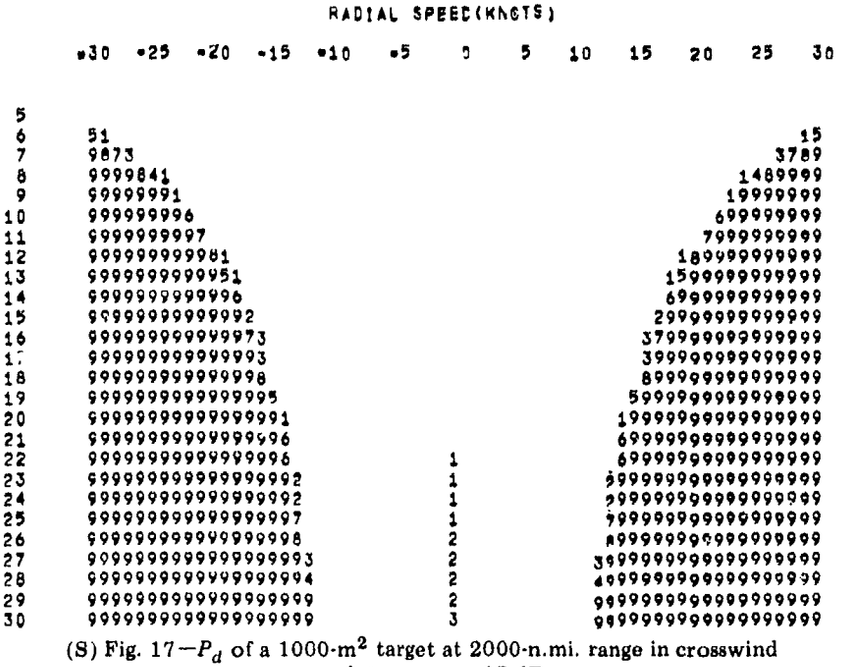

(S) Fig. 17—P_d of a 1000-m^2 target at 2000-n.mi. range in crosswind sea clutter, σ_0 = -17 dB

RADIAL SPEED(KNOTS)

	-30	-25	-20	-15	-10	-5	0	5	10	15	20	25	30
5	99961						37973					16999	
6	99999883						1599951					38899999	
7	9999999951						1699961					1599999999	
8	999999999961						3899983					1699999999999	
9	9999999999972						4999994					2799999999999	
10	99999999999984						99999					48999999999999	
11	999999999999991						1699961					199999999999999	
12	9999999099999961						1799971					1699999999999999	
13	99999999999999996						1899981					6999999999999999	
14	99999999999999992						2999992					29999999999999999	
15	99999999999999998						3999993					89999999999999999	
16	999999999999999984						99999					489999999999999999	
17	9999999999999999991						99999					1999999999999999999	
18	9999999999999999995						99999					5999999999999999999	
19	9999999999999999996						99999					6999999999999999999	
20	99999999999999999992						99999					29999999999999999999	
21	99999999999999999992						1699961					29999999999999999999	
22	99999999999999999997						1799971					79999999999999999999	
23	99999999999999999998						79997					89999999999999999999	
24	999999999999999999994						89998					499999999999999999999	
25	999999999999999999994						89998					499999999999999999999	
26	999999999999999999999						99999					999999999999999999999	
27	999999999999999999999						99999					999999999999999999999	
28	999999999999999999999						99999					999999999999999999999	
29	9999999999999999999996						99999					6999999999999999999999	
30	9999999999999999999996						99999					6999999999999999999999	

(S) Fig. 18—P_d of a 3000-m^2 target at 500-n.mi. range in crosswind sea clutter, σ_0 = -17 dB

RADIAL SPEED(KNOTS)

	-30	-25	-20	-15	-10	-5	0	5	10	15	20	25	30
5	994						131					499	
6	9999611						252					1169999	
7	99999982						363					28999999	
8	9999999994						15851					4999999999	
9	99999999951						26962					159999999999	
10	9999999999961						37973					1699999999999	
11	99999999999972						898					27999999999999	
12	99999999999998						19991					89999999999999	
13	99999999999994						19991					49999999999999	
14	99999999999999994						19991					49999999999999999	
15	99999999999999951						29992					159999999999999999	
16	99999999999999991						38983					199999999999999999	
17	99999999999999962						38983					369999999999999999	
18	99999999999999992						49994					999999999999999999	
19	99999999999999998						49994					899999999999999999	
20	999999999999999983						59995					3899999999999999999	
21	999999999999999994						999					4999999999999999999	
22	9999999999999999991						999					1999999999999999999	
23	9999999999999999991						19991					1999999999999999999	
24	9999999999999999995						19991					5999999999999999999	
25	9999999999999999996						19991					6999999999999999999	
26	99999999999999999992						19991					29999999999999999999	
27	99999999999999999992						29992					29999999999999999999	
28	99999999999999999992						29992					29999999999999999999	
29	99999999999999999997						29992					79999999999999999999	
30	99999999999999999998						39993					89999999999999999999	

(S) Fig. 19—P_d of a 3000-m^2 target at 1000-n.mi. range in crosswind sea clutter, σ_0 = -17 dB

RADIAL SPEED(KNOTS)

	-30	-25	-20	-15	-10	-5	0	5	10	15	20	25	30
5	551												159
6	9972						1						27999
7	9999993						2						3999999
8	999999951						141						1599999999
9	999999961						252						16999999999
10	99999999972						363						279999999999
11	999999999983						474						3899999999999
12	9999999999994						585						49999999999999
13	99999999999999						696						999999999999999
14	9999999999999961						696						16999999999999999
15	9999999999999991						797						19999999999999999
16	9999999999999997						494						79999999999999999
17	99999999999999992						494						29999999999999999
18	99999999999999998						15951						89999999999999999
19	999999999999999993						15951						99999999999999999
20	999999999999999994						16961						49999999999999999
21	9999999999999999991						696						199999999999999999
22	9999999999999999995						797						599999999999999999
23	9999999999999999996						797						599999999999999999
24	99999999999999999991						898						199999999999999999
25	99999999999999999992						898						299999999999999999
26	99999999999999999997						999						799999999999999999
27	99999999999999999997						999						799999999999999999
28	99999999999999999997						999						799999999999999999
29	999999999999999999993						999						399999999999999999999
30	999999999999999999994						999						499999999999999999999

(S) Fig. 20—P_d of a 3000-m^2 target at 1500-n.mi. range in crosswind sea clutter, σ_0 = -17 dB

RADIAL SPEED(KNOTS)

	-30	-25	-20	-15	-10	-5	0	5	10	15	20	25	30
5	62												26
6	9984												4899
7	9999961												1699999
8	999999972						1						279999999
9	9999999983						2						3899999999
10	99999999994						131						49999999999
11	99999999999951						141						1599999999999
12	99999999999961						252						16999999999999
13	99999999999997						363						799999999999999
14	999999999999982						363						2899999999999999
15	999999999999998						474						8999999999999999
16	9999999999999994						181						49999999999999999
17	9999999999999999						181						99999999999999999
18	99999999999999995						292						599999999999999999
19	999999999999999961						292						1699999999999999999
20	999999999999999991						393						1999999999999999999
21	999999999999999997						393						7999999999999999999
22	9999999999999999972						494						27999999999999999999
23	9999999999999999992						494						29999999999999999999
24	9999999999999999998						595						89999999999999999999
25	9999999999999999999						595						99999999999999999999
26	99999999999999999994						696						499999999999999999999
27	99999999999999999994						696						499999999999999999999
28	99999999999999999995						696						599999999999999999999
29	999999999999999999991						797						1999999999999999999999
30	999999999999999999991						797						1999999999999999999999

(S) Fig. 21—P_d of a 3000-m^2 target at 2000-n.mi. range in crosswind sea clutter, σ_0 = -17 dB

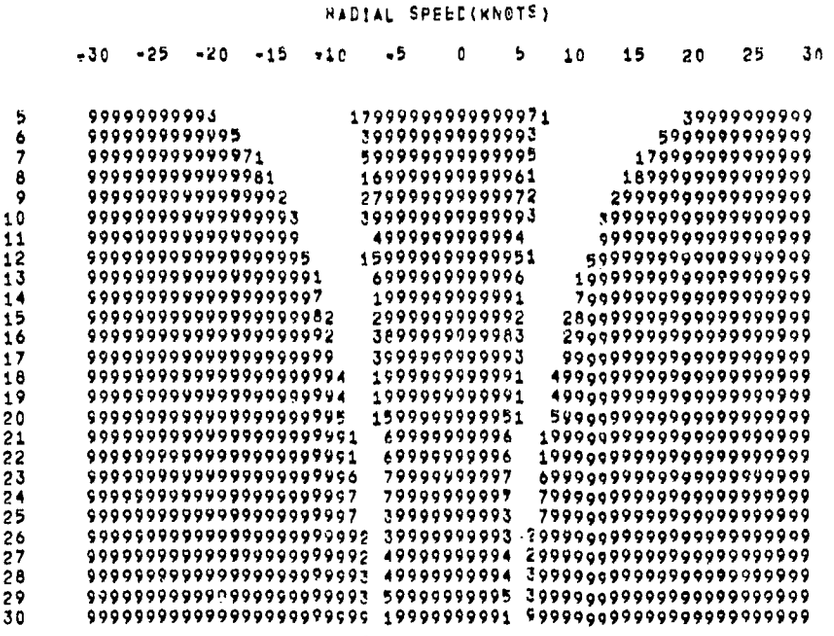

(S) Fig. 22—P_d of a 50,000-m^2 target at 500-n.mi. range in crosswind sea clutter, σ_0 = -17 dB

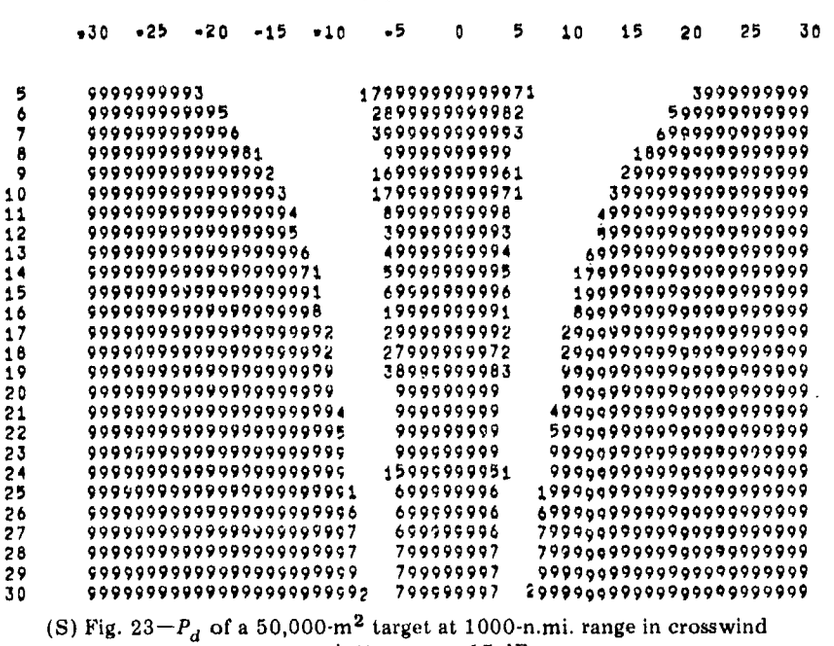

(S) Fig. 23—P_d of a 50,000-m^2 target at 1000-n.mi. range in crosswind sea clutter, σ_0 = -17 dB

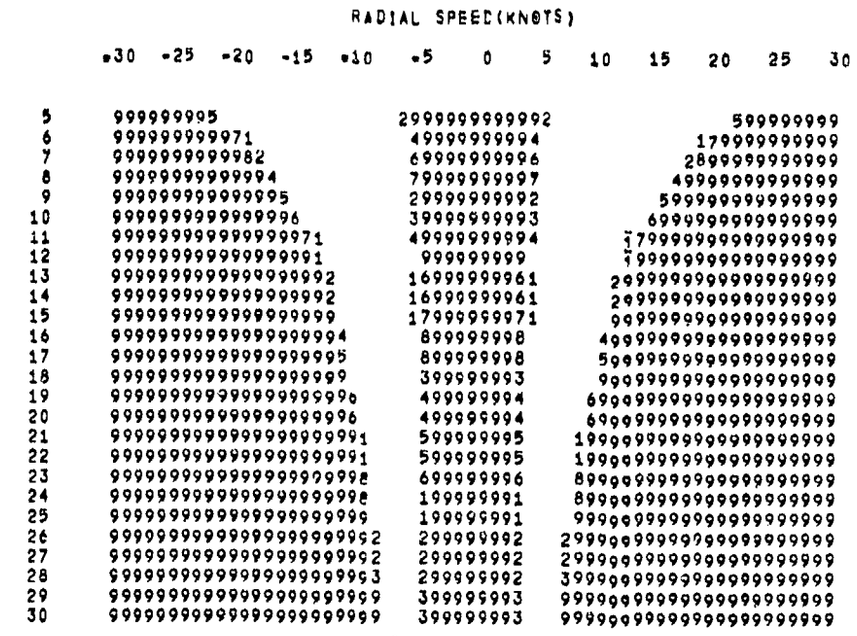

(S) Fig. 24—P_d of a 50,000-m^2 target at 1500-n.mi. range in crosswind sea clutter, σ_0 = -17 dB

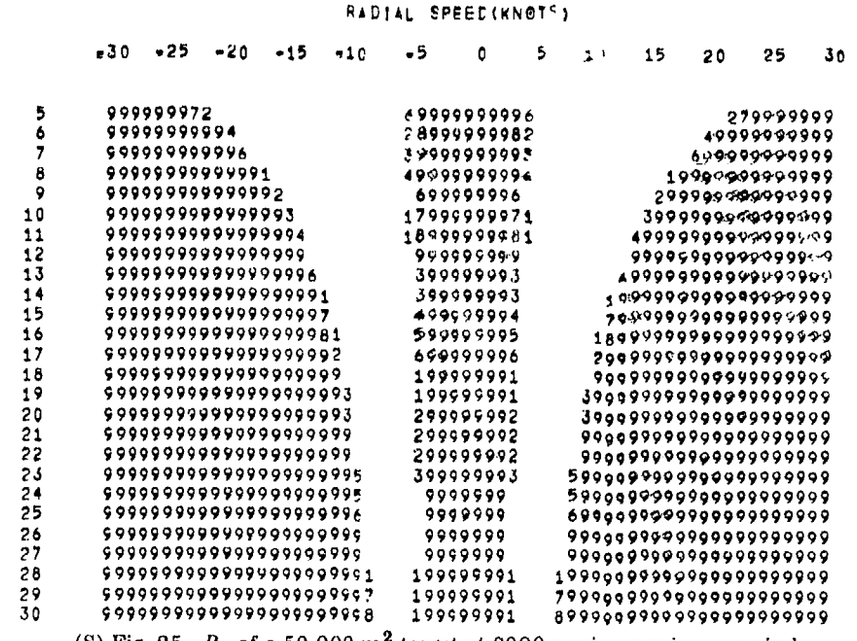

(S) Fig. 25—P_d of a 50,000-m^2 target at 2000-n.mi. range in crosswind sea clutter, σ_0 = -17 dB

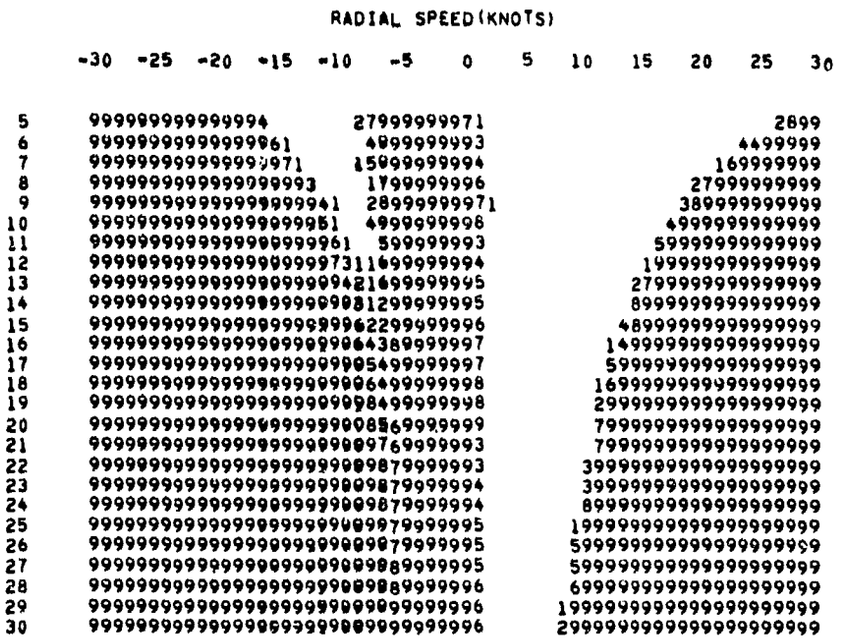

(S) Fig. 26—P_d of a 1000-m^2 target at 500-n.mi. range in approaching sea clutter, σ_0 = -23 dB

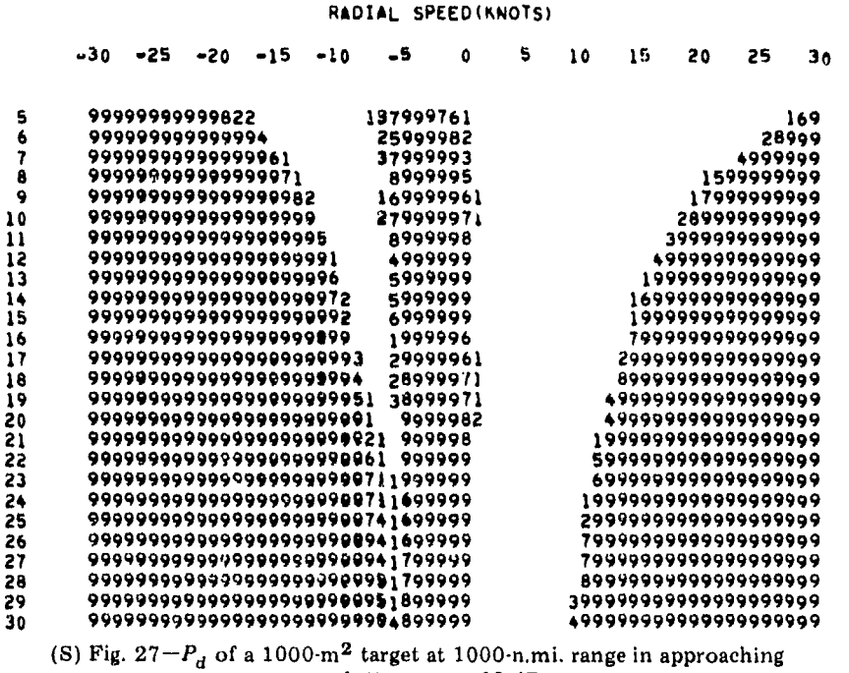

(S) Fig. 27—P_d of a 1000-m^2 target at 1000-n.mi. range in approaching sea clutter, σ_0 = -23 dB

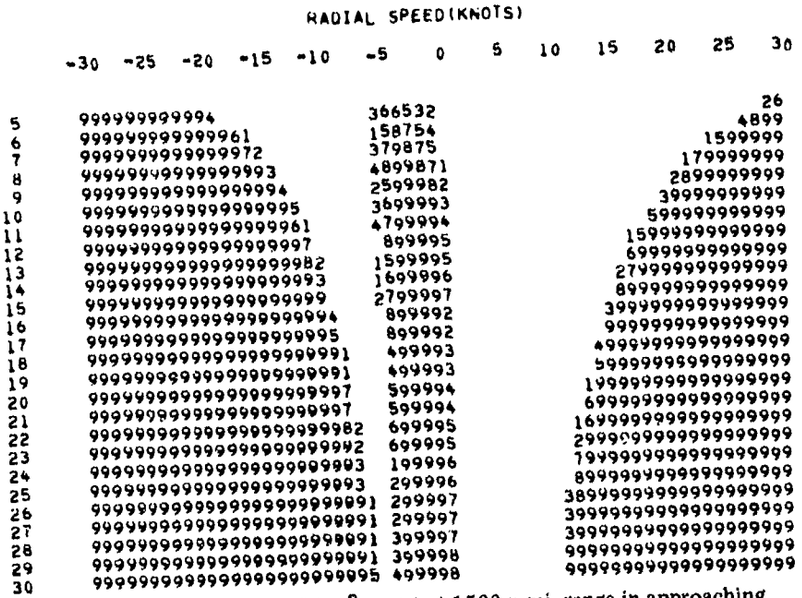

(S) Fig. 28—P_d of a 1000-m^2 target at 1500-n.mi. range in approaching sea clutter, σ_0 = -23 dB

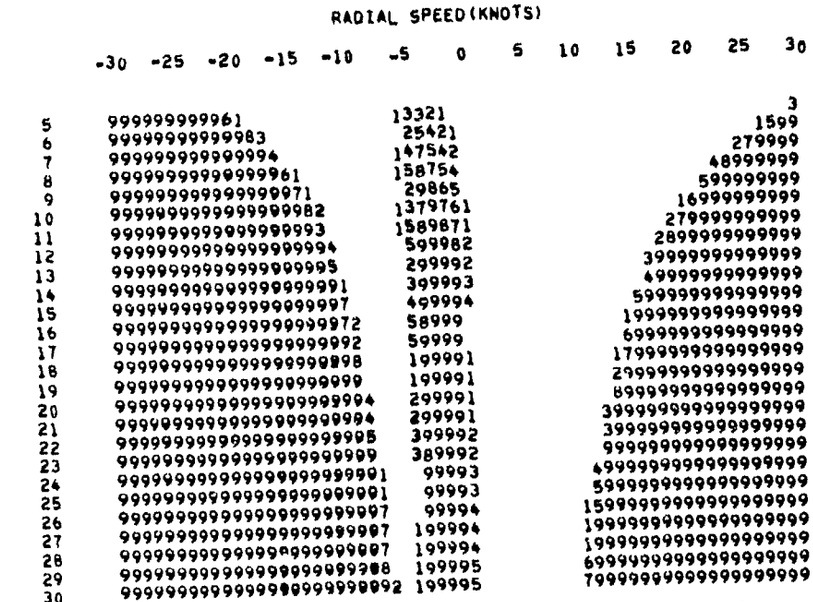

(S) Fig. 29—P_d of a 1000-m^2 target at 2000-n.mi. range in approaching sea clutter, σ_0 = -23 dB

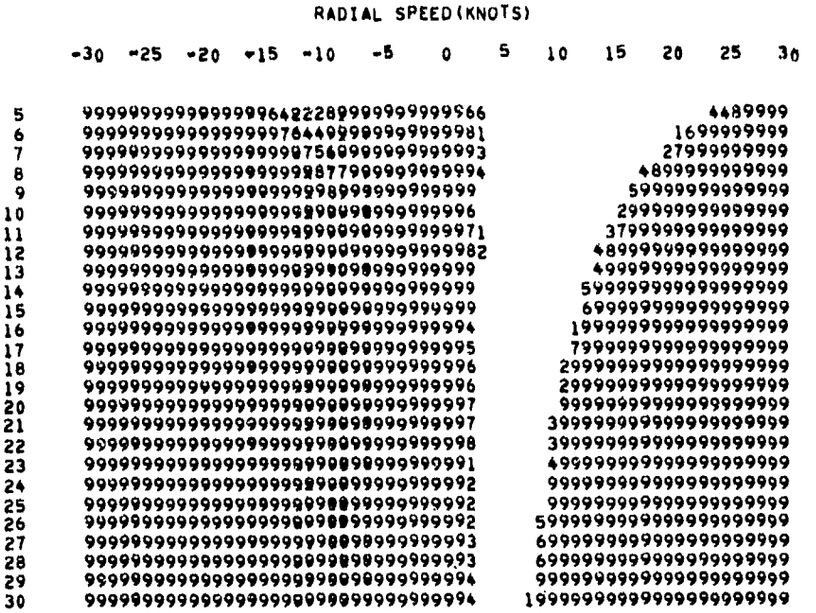

(S) Fig. 30—P_d of a 3000-m^2 target at 500-n.mi. range in approaching sea clutter, σ_0 = -23 dB

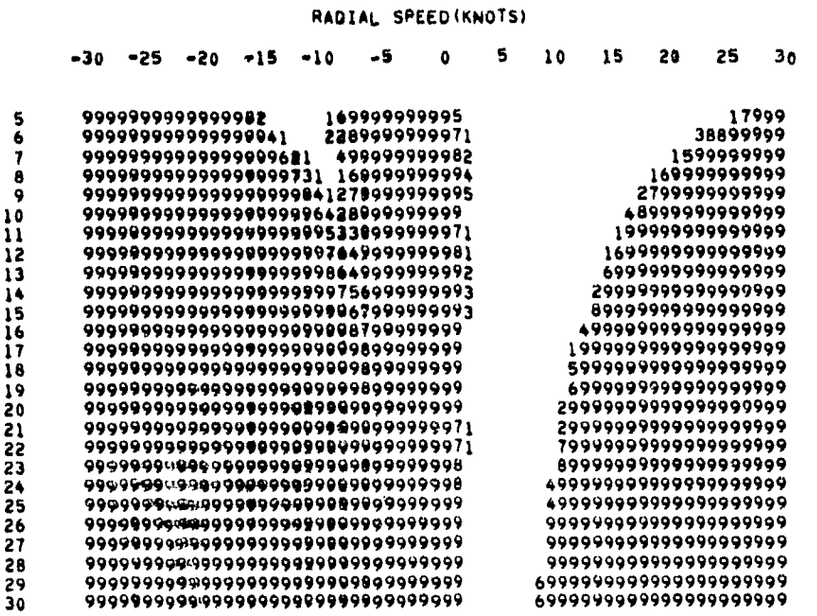

(S) Fig. 31—P_d of a 3000-m^2 target at 1000-n.mi. range in approaching sea clutter, σ_0 = -23 dB

RADIAL SPEED(KNOTS)

	-30	-25	-20	-15	-10	-5	0	5	10	15	20	25	30
5	9999999999999994					87999999971							2899
6	99999999999999961					4999999993							4499999
7	99999999999999972					15999999994							169999999
8	99999999999999999993					1799999996							27999999999
9	999999999999999999941					28999999971							389999999999
10	999999999999999999951					4899999998							4999999999999
11	999999999999999999961					599999993							59999999999999
12	9999999999999999999973					11699999994							199999999999999
13	9999999999999999999994					21699999995							2799999999999999
14	9999999999999999999993					1299999995							8999999999999999
15	9999999999999999999999962					299999996							48999999999999999
16	9999999999999999999999964					399999997							149999999999999999
17	9999999999999999999999954					499999997							599999999999999999
18	9999999999999999999999964					999999998							1699999999999999999
19	9999999999999999999999984					499999999							2999999999999999999
20	9999999999999999999999995					69999999							7999999999999999999
21	9999999999999999999999997					69999993							7999999999999999999
22	9999999999999999999999998					79999993							39999999999999999999
23	9999999999999999999999998					79999994							49999999999999999999
24	9999999999999999999999997					79999994							99999999999999999999
25	9999999999999999999999998					79999995							199999999999999999999
26	9999999999999999999999997					79999995							599999999999999999999
27	9999999999999999999999998					89999995							599999999999999999999
28	9999999999999999999999998					89999996							699999999999999999999
29	9999999999999999999999999					99999996							1999999999999999999999
30	9999999999999999999999999					99999997							2999999999999999999999

(S) Fig. 32—P_d of a 3000-m^2 target at 1500-n.mi. range in approaching sea clutter, σ_0 = -23 dB

RADIAL SPEED(KNOTS)

	-30	-25	-20	-15	-10	-5	0	5	10	15	20	25	30
5	999999999999771					489999994							599
6	9999999999999983					1699999961							1179999
7	999999999999999994					2799999981							38999999
8	999999999999999961					499999993							4999999999
9	9999999999999999971					1599999994							169999999999
10	9999999999999999992					1699999995							1799999999999
11	9999999999999999993					299999991							28999999999999
12	9999999999999999999941					3899999991							89999999999999
13	9999999999999999999991					399999992							4999999999999999
14	9999999999999999999961					99999992							5999999999999999
15	9999999999999999999973					199999993							16999999999999999
16	9999999999999999999993					1169999994							29999999999999999
17	9999999999999999999999821					69999995							279999999999999999
18	9999999999999999999999831					79999995							399999999999999999
19	9999999999999999999999951					79999996							899999999999999999
20	9999999999999999999999962					39999996							4899999999999999999
21	9999999999999999999999964					39999991							4999999999999999999
22	9999999999999999999999995					49999991							19999999999999999999
23	9999999999999999999999995					49999991							19999999999999999999
24	9999999999999999999999965					59999991							69999999999999999999
25	9999999999999999999999984					59999992							69999999999999999999
26	9999999999999999999999985					59999992							299999999999999999999
27	9999999999999999999999995					59999992							299999999999999999999
28	9999999999999999999999995					59999993							399999999999999999999
29	9999999999999999999999996					69999993							899999999999999999999
30	9999999999999999999999998					89999994							899999999999999999999

(S) Fig. 33—P_d of a 3000-m^2 target at 2000-n.mi. range in approaching sea clutter, σ_0 = -23 dB

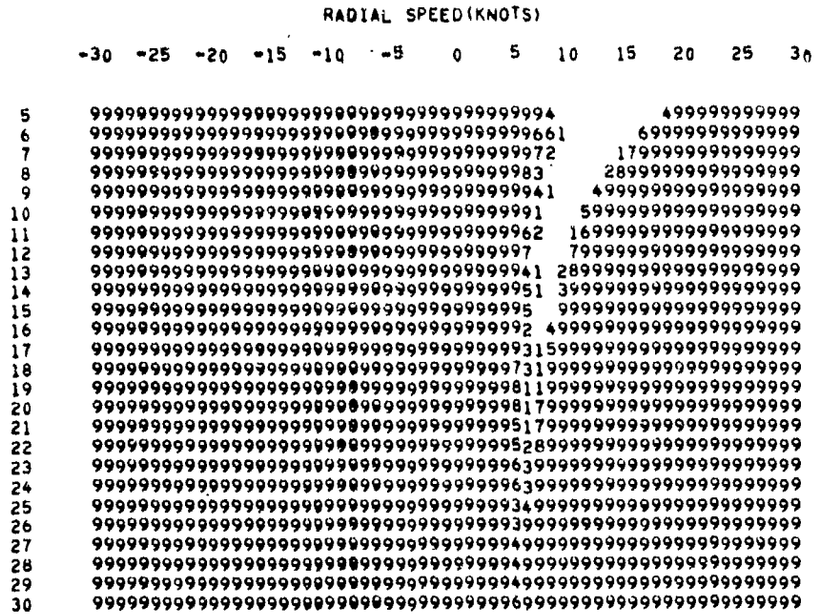

(S) Fig. 34—P_d of a 50,000-m^2 target at 500-n.mi. range in approaching sea clutter, σ_0 = -23 dB

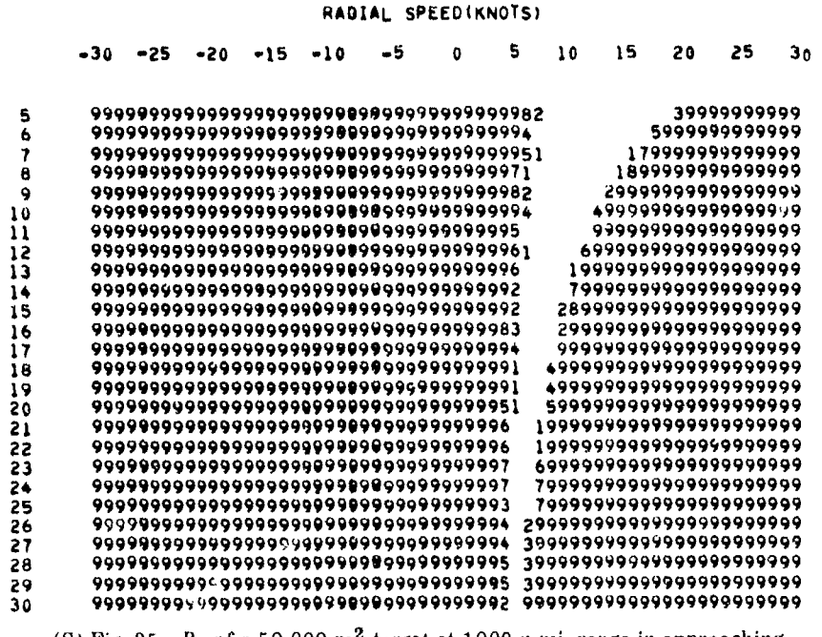

(S) Fig. 35—P_d of a 50,000-m^2 target at 1000-n.mi. range in approaching sea clutter, σ_0 = -23 dB

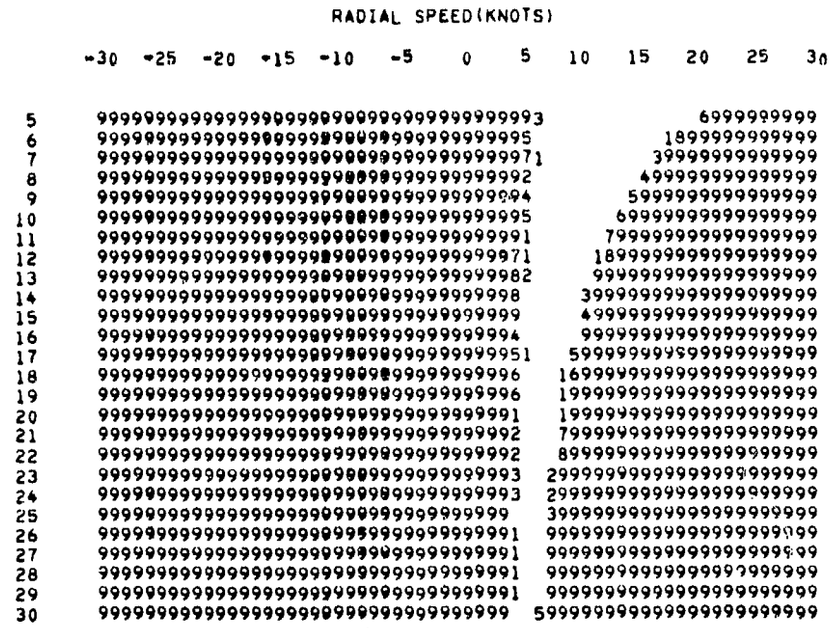

(S) Fig. 36—P_d of a 50,000-m^2 target at 1500-n.mi. range in approaching sea clutter, σ_0 = -23 dB

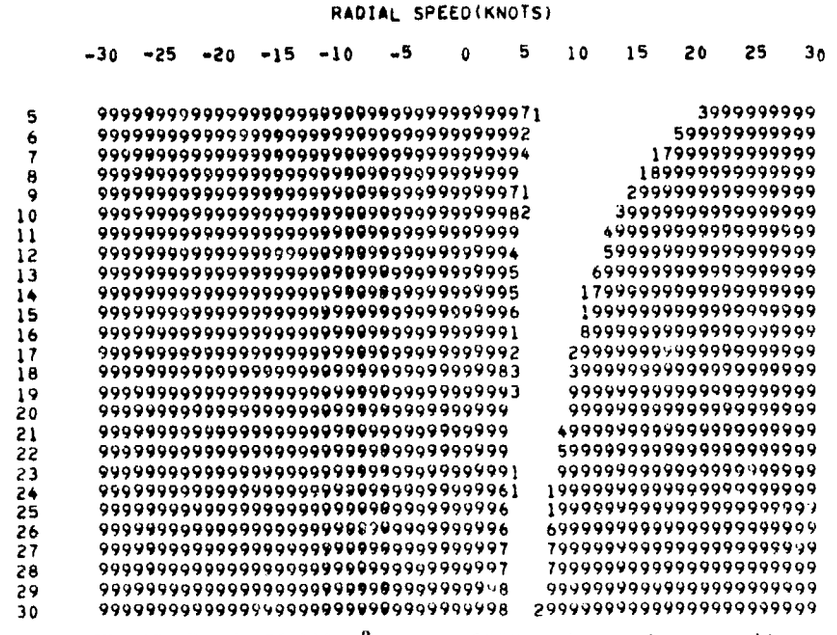

(S) Fig. 37 -P_d of a 50,000-m^2 target at 2000-n.mi. range in approaching sea clutter, σ_0 = -23 dB

RADIAL SPEED(KNOTS)

	-30	-25	-20	-15	-10	-5	0	5	10	15	20	25	30
5	99994					116999611						49999	
6	999999961					3899983						1609999999	
7	9999999973					4999994						3799999999	
8	999999999994					6999996						4999999999	
9	99999999999951					7999997						15999999999999	
10	999999999999997					2999992						79999999999999	
11	9999999999999993					2999992						399999999999999	
12	9999999999999984					3999993						489999999999999	
13	99999999999999991					4999994						1999999999999999	
14	999999999999999951					5999995						15999999999999999	
15	999999999999999992					6999996						29999999999999999	
16	999999999999999997					1999991						79999999999999999	
17	9999999999999999993					1999991						399999999999999999	
18	99999999999999999998					1999991						899999999999999999	
19	999999999999999999					2999992						999999999999999999	
20	9999999999999999995					2999992						5999999999999999999	
21	9999999999999999995					2999992						5999999999999999999	
22	9999999999999999999					3999993						9999999999999999999	
23	99999999999999999991					99999						19999999999999999999	
24	99999999999999999996					99999						69999999999999999999	
25	99999999999999999997					99999						79999999999999999999	
26	99999999999999999991					99999						19999999999999999999	
27	99999999999999999999					99999						19999999999999999999	
28	99999999999999999992					99999						29999999999999999999	
29	99999999999999999998					99999						89999999999999999999	
30	99999999999999999999					99999						99999999999999999999	

(S) Fig. 38—P_d of a 1000-m^2 target at 500-n.mi. range in crosswind sea clutter, σ_0 = -23 dB

RADIAL SPEED(KNOTS)

	-30	-25	-20	-15	-10	-5	0	5	10	15	20	25	30
5	9972						363					2799	
6	9999944						15851					4499999	
7	999999951						26962					159999999	
8	99999999972						38983					27999999999	
9	999999999983						1599951					389999999999	
10	9999999999994						69996					4999999999999	
11	99999999999995						29992					59999999999999	
12	999999999999991						39993					199999999999999	
13	9999999999999972						39993					2799999999999999	
14	9999999999999997						49994					7999999999999999	
15	99999999999999983						59995					38999999999999999	
16	99999999999999941						69996					149999999999999999	
17	9999999999999999995						69996					599999999999999999	
18	99999999999999999951						79997					1599999999999999999	
19	999999999999999999991						79997					1999999999999999999	
20	999999999999999999997						89998					7999999999999999999	
21	999999999999999999997						29992					7999999999999999999	
22	999999999999999999993						29992					3999999999999999999	
23	999999999999999999993						39993					3999999999999999999	
24	999999999999999999998						39993					8999999999999999999	
25	999999999999999999991						49994					1999999999999999999	
26	999999999999999999995						49994					5999999999999999999	
27	999999999999999999995						59995					5999999999999999999	
28	999999999999999999995						59995					5999999999999999999	
29	999999999999999999991						59995					1999999999999999999	
30	999999999999999999992						69996					2999999999999999999	

(S) Fig. 39—P_d of a 1000-m^2 target at 1000-n.mi. range in crosswind sea clutter, σ_0 = -23 dB

RADIAL SPEED (KNOTS)

	-30	-25	-20	-15	-10	-5	0	5	10	15	20	25	30
5	983						2						389
6	9999511						141						1159999
7	99999971						252						17999999
8	9999999983						474						3899999999
9	99999999994						15851						49999999999
10	9999999999951						26962						1599999999999
11	99999999999961						797						16999999999999
12	999999999999997						898						79999999999999
13	9999999999999992						999						299999999999999
14	99999999999999983						19991						3899999999999999
15	99999999999999994						19991						4999999999999999
16	999999999999999991						27972						19999999999999999
17	999999999999999951						27972						15999999999999999
18	999999999999999991						38983						19999999999999999
19	999999999999999996						38983						69999999999999999
20	9999999999999999972						49994						279999999999999999
21	9999999999999999993						999						399999999999999999
22	9999999999999999998						999						899999999999999999
23	9999999999999999998						999						899999999999999999
24	99999999999999999994						999						4999999999999999999
25	99999999999999999998						19991						5999999999999999999
26	999999999999999999991						19991						19999999999999999999
27	999999999999999999991						19991						19999999999999999999
28	999999999999999999991						19991						19999999999999999999
29	999999999999999999996						19991						69999999999999999999
30	9999999999999999999997						29992						79999999999999999999

(S) Fig. 40—P_d of a 1000-m^2 target at 1500-n.mi. range in crosswind sea clutter, σ_0 = -23 dB

RADIAL SPEED (KNOTS)

	-30	-25	-20	-15	-10	-5	0	5	10	15	20	25	30
5	951												159
6	99972						1						27999
7	9999994						2						4999999
8	9999999951						141						1599999999
9	99999999961						252						16999999999
10	999999999972						363						279999999999
11	9999999999983						474						3899999999999
12	99999999999994						585						49999999999999
13	99999999999999						696						99999999999999
14	9999999999999961						696						16999999999999999
15	9999999999999991						797						19999999999999999
16	9999999999999997						494						79999999999999999
17	99999999999999992						494						29999999999999999
18	99999999999999998						15951						89999999999999999
19	999999999999999993						15951						39999999999999999999
20	999999999999999994						16961						49999999999999999999
21	9999999999999999991						696						19999999999999999999
22	9999999999999999995						797						59999999999999999999
23	9999999999999999996						797						69999999999999999999
24	99999999999999999991						898						19999999999999999999
25	99999999999999999992						898						29999999999999999999
26	99999999999999999997						999						79999999999999999999
27	99999999999999999997						999						79999999999999999999
28	99999999999999999998						999						89999999999999999999
29	999999999999999999993						999						399999999999999999999
30	999999999999999999994						999						499999999999999999999

(S) Fig. 41—P_d of a 1000-m^2 target at 2000-n.mi. range in crosswind sea clutter, σ_0 = -23 dB

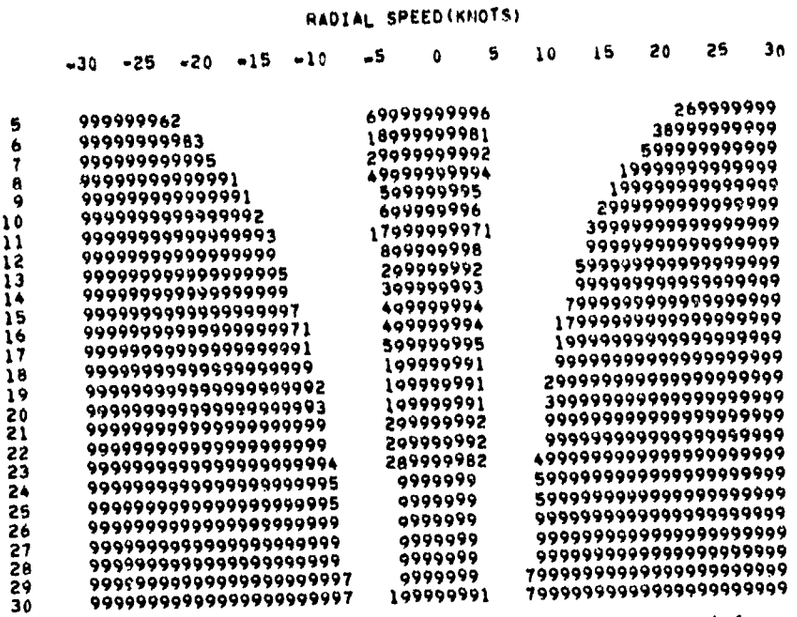

(S) Fig. 42—P_d of a 3000-m^2 target at 500-n.mi. range in crosswind sea clutter, σ_0 = -23 dB

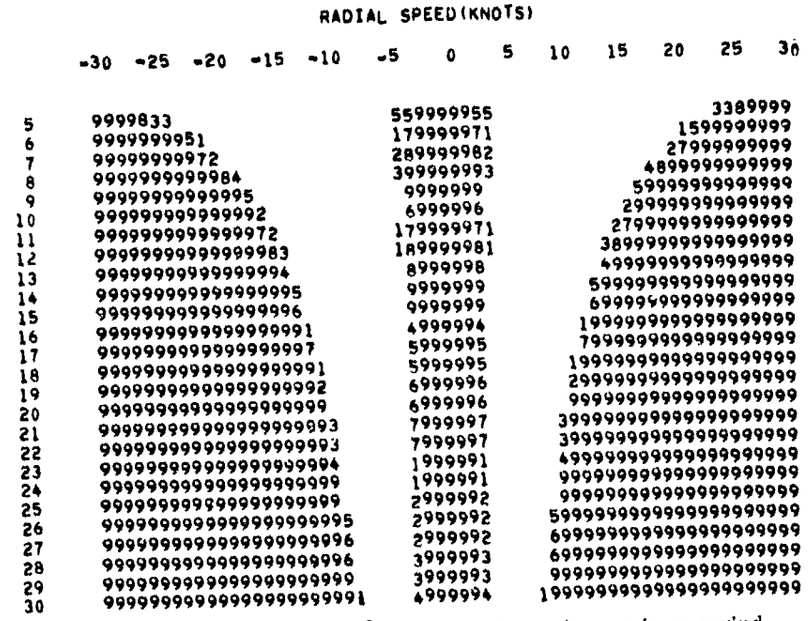

(S) Fig. 43—P_d of a 3000-m^2 target at 1000-n.mi. range in crosswind sea clutter, σ_0 = -23 dB

RADIAL SPEED(KNOTS)

	-30	-25	-20	-15	-10	-5	0	5	10	15	20	25	30
5	99994					116999611						49999	
6	999999961					3899983						169999999	
7	9999999973					4999994						3799999999	
8	9999999999941					6999996						14999999999999	
9	99999999999951					7999997						159999999999999	
10	999999999999997					2999992						799999999999999	
11	9999999999999993					2999992						3999999999999999	
12	99999999999999984					3999993						48999999999999999	
13	999999999999999991					4999994						199999999999999999	
14	9999999999999999951					5999995						1599999999999999999	
15	9999999999999999992					6999996						2999999999999999999	
16	9999999999999999997					1999991						7999999999999999999	
17	99999999999999999993					1999991						39999999999999999999	
18	99999999999999999998					1999991						89999999999999999999	
19	99999999999999999999					2999992						99999999999999999999	
20	99999999999999999995					2999992						59999999999999999999	
21	99999999999999999995					2999992						59999999999999999999	
22	99999999999999999999					3999993						99999999999999999999	
23	999999999999999999991					99999						199999999999999999999	
24	999999999999999999997					99999						799999999999999999999	
25	999999999999999999997					99999						799999999999999999999	
26	999999999999999999991					99999						199999999999999999999	
27	999999999999999999992					99999						299999999999999999999	
28	999999999999999999992					99999						299999999999999999999	
29	999999999999999999998					99999						899999999999999999999	
30	999999999999999999999					99999						999999999999999999999	

(S) Fig. 44—P_d of a 3000-m^2 target at 1500-n.mi. range in crosswind sea clutter, σ_0 = -23 dB

RADIAL SPEED(KNOTS)

	-30	-25	-20	-15	-10	-5	0	5	10	15	20	25	30
5	99961					37973						16999	
6	99999883					1599951						38899999	
7	9999999941					1699961						1499999999	
8	999999999961					3899983						169999999999	
9	9999999999972					4999994						2799999999999	
10	99999999999983					99999						389999999999999	
11	999999999999991					69996						1999999999999999	
12	9999999999999951					1799971						15999999999999999	
13	9999999999999996					1899981						69999999999999999	
14	9999999999999992					2899982						29999999999999999	
15	9999999999999998					3999993						89999999999999999	
16	99999999999999984					99999						489999999999999999	
17	999999999999999991					99999						1999999999999999999	
18	999999999999999995					99999						5999999999999999999	
19	999999999999999996					99999						6999999999999999999	
20	9999999999999999992					99999						2999999999999999999	
21	999999999999999992					69996						2999999999999999999	
22	9999999999999999997					1799971						7999999999999999999	
23	99999999999999999998					79997						8999999999999999999	
24	999999999999999999993					89998						3999999999999999999	
25	999999999999999999994					89998						4999999999999999999	
26	999999999999999999999					89998						9999999999999999999	
27	999999999999999999999					99999						9999999999999999999	
28	999999999999999999999					99999						9999999999999999999	
29	999999999999999999995					99999						5999999999999999999	
30	999999999999999999996					99999						6999999999999999999	

(S) Fig. 45—P_d of a 3000-m^2 target at 2000-n.mi. range in crosswind sea clutter, σ_0 = -23 dB

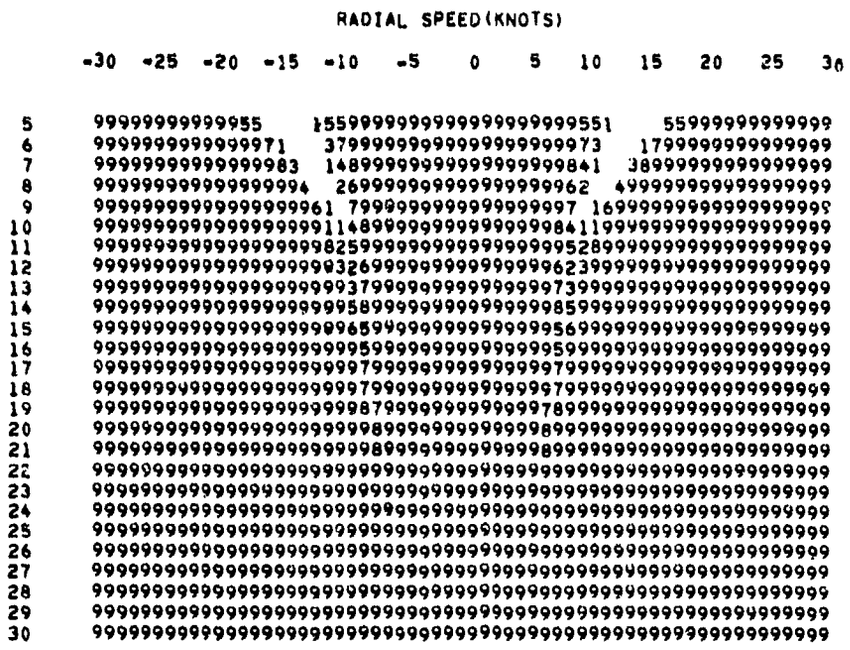

(S) Fig. 46—P_d of a 50,000-m^2 target at 500-n.mi. range in crosswind sea clutter, σ_0 = -23 dB

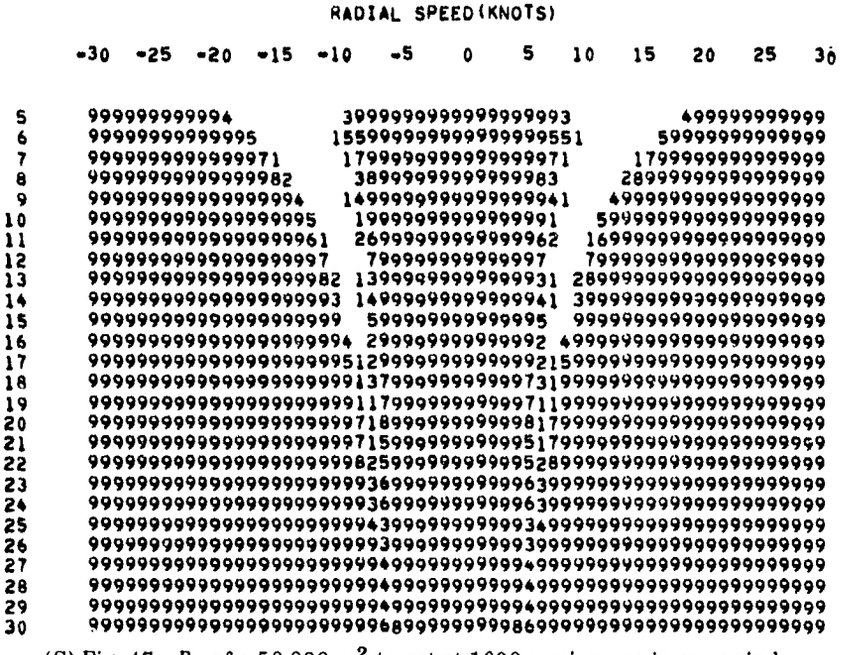

(S) Fig. 47—P_d of a 50,000-m^2 target at 1000-n.mi. range in crosswind sea clutter, σ_0 = -23 dB

RADIAL SPEED(KNOTS)

	-30	-25	-20	-15	-10	-5	0	5	10	15	20	25	30
5	99999999996					49999999999999994							69999999999
6	99999999999981					1169999999999999611							189999999999999
7	999999999999993					28899999999999982							3999999999999999
8	99999999999999994					4999999999999994							49999999999999999
9	999999999999999996					15999999999999951							699999999999999999
10	9999999999999999971					6999999999999996							1799999999999999999
11	99999999999999999992					2799999999999972							2999999999999999999
12	999999999999999999982					3899999999999983							2899999999999999999
13	999999999999999999993					99999999999999							3999999999999999999
14	999999999999999999999					1499999999999941							999999999999999999999
15	9999999999999999999995					1599999999999951							599999999999999999999
16	99999999999999999999961					69999999999996							1699999999999999999999
17	99999999999999999999991					6999999999996							1999999999999999999999
18	99999999999999999999997					3999999999993							7999999999999999999999
19	99999999999999999999997					3999999999993							7999999999999999999999
20	999999999999999999999982					4899999999984							2899999999999999999999
21	99999999999999999999993					1999999999991							3999999999999999999999
22	99999999999999999999993					1999999999991							3999999999999999999999
23	99999999999999999999999					2999999999992							9999999999999999999999
24	99999999999999999999999					2999999999992							9999999999999999999999
25	99999999999999999999999					699999999996							9999999999999999999999
26	999999999999999999999995					79999999997							5999999999999999999999
27	999999999999999999999996					79999999997							6999999999999999999999
28	9999999999999999999999961					7999999999971							6999999999999999999999
29	9999999999999999999999961					8999999999981							6999999999999999999999
30	9999999999999999999999991					4999999999941							9999999999999999999999

(S) Fig. 48—P_d of a 50,000-m^2 target at 1500-n.mi. range in crosswind sea clutter, σ_0 = -23 dB

RADIAL SPEED(KNOTS)

	-30	-25	-20	-15	-10	-5	0	5	10	15	20	25	30
5	99999999993					27999999999999972							39999999999
6	99999999995					3999999999999993							59999999999
7	999999999999971					15999999999999951							179999999999999
8	999999999999981					1699999999999961							1899999999999999
9	99999999999999992					2899999999999982							2999999999999999
10	999999999999999994					3999999999999993							4999999999999999999
11	99999999999999999					49999999999994							99999999999999999999
12	999999999999999999961					1599999999999951							1699999999999999999999
13	999999999999999999991					69999999999996							1999999999999999999999
14	999999999999999999997					29999999999992							7999999999999999999999
15	9999999999999999999982					29999999999992							2899999999999999999999
16	99999999999999999999992					38999999999983							2999999999999999999999
17	99999999999999999999999					39999999999993							9999999999999999999999
18	999999999999999999999994					19999999999991							4999999999999999999999
19	999999999999999999999994					19999999999991							4999999999999999999999
20	999999999999999999999995					15999999999951							5999999999999999999999
21	9999999999999999999999991					699999999996							1999999999999999999999
22	9999999999999999999999991					699999999996							1999999999999999999999
23	99999999999999999999999996					799999999997							6999999999999999999999
24	99999999999999999999999997					799999999997							7999999999999999999999
25	99999999999999999999999997					399999999993							7999999999999999999999
26	999999999999999999999999992					499999999994							2999999999999999999999
27	999999999999999999999999993					499999999994							3999999999999999999999
28	999999999999999999999999993					499999999994							3999999999999999999999
29	999999999999999999999999993					599999999995							3999999999999999999999
30	999999999999999999999999999					199999999991							9999999999999999999999

(S) Fig. 49—P_d of a 50,000-m^2 target at 2000-n.mi. range in crosswind sea clutter, σ_0 = -23 dB

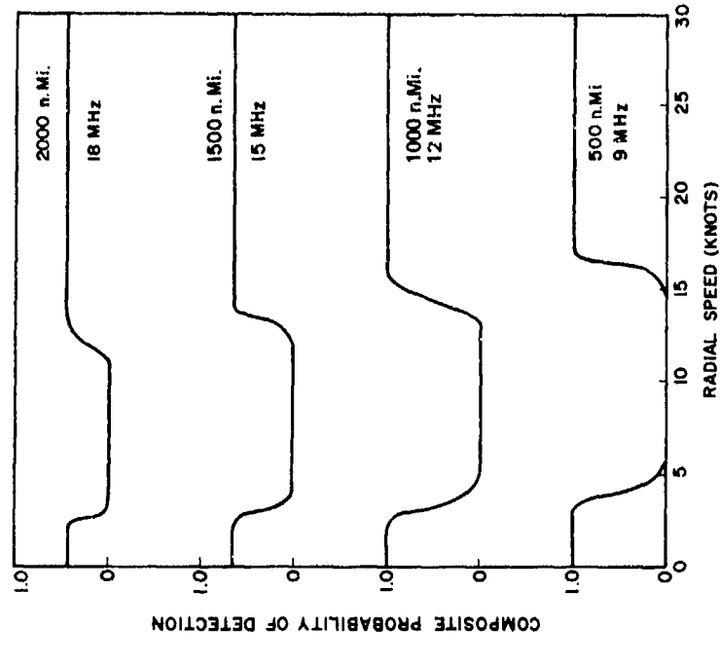

(S) Fig. 51—Composite P_d of a 3000-mi^2 target in crosswind sea clutter, $\sigma_0 = -23$ dB

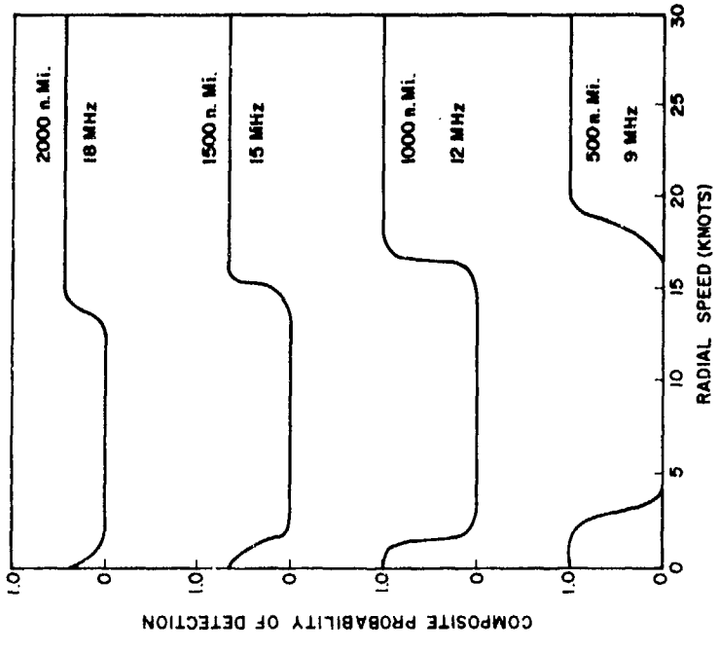

(S) Fig. 50—Composite P_d of a 3000-m^2 target in crosswind sea clutter, $\sigma_0 = -17$ dB

below 13 knots if σ_0 = -23 dB. The composite P_d's are limited at long ranges by the probability of propagation. Thus, the composite P_d would be raised by any feature which improves propagation, such as allowing multiple-bounce propagation or increasing power.

ACKNOWLEDGMENTS

(U) I would like to thank Dr. G. V. Trunk for his assistance in formulating the criteria for propagation, and Dr. J. R. Barnum for the advanced copy of sea clutter data and his helpful remarks concerning the nature of sea clutter.

REFERENCES

1. H.L. Stalford, "A Minimum-Distance Method for Ocean Surveillance Resolution," NRL Report 7677, Mar. 22, 1974.
2. H.L. Stalford, "A Combinatorial Occupancy Method for Determining Parameter Resolution in a Multi-Target Environment," NRL Report 7702, May 1, 1974.
3. H.L. Stalford, "Solitary Occupancy for Unequal Cell Probabilities with Application to Doppler Radars for Ocean Surveillance," NRL Report 7708, May 20, 1974.
4. H.L. Stalford, "Probability That *N* ships in an Ocean Surveillance Range-Azimuth Cell Occupy Separate Doppler Bins," NRL Report 7715, May 22, 1974.
5. H.L. Stalford, "Probability of Resolving *N* Ships From Radar Observations," NRL Report 7726, May 23, 1974.
6. W.B. Gordon, "Cost Analysis of an OTH Radar System," NRL Report 7752, pending publication.
7. J.M. Headrick, J.F. Thomason, DlL. Lucas, S.R. McCammon, R.A. Hanson, and J.L. Lloyd, "Virtual Path Tracing for HF Radar Including an Ionospheric Model," NRL Memorandum Report 2226, Mar. 29, 1971.
8. W.L. Rubin and J.V. Difranco, "Radar Detection," *Electro-Tech., Sci. Eng. Ser.* 64, 61-91 (Apr. 1964).
9. J.R. Barnum, "Assorted Sea-Clutter and Single-Signal Spectra Contents and Notes," Stanford Research Institute, Oct. 17, 1973.
10. A.E. Long and D.B. Trizna, "Mapping of North Atlantic Winds by HF Radar Sea Backscatter Interpretation," *IEEE Trans. Antennas and Propagation*, AP-21 (No. 5), (Sept. 1973).
11. M.I. Skolnik, editor, *Radar Handbook*, McGraw-Hill, New York, 1970, Chap. 26.
12. J.R. Barnum, "Ship Ahoy Through March 1973," *Proceedings of the OHD Technical Review Meeting* of May 2-3, 1973, Vol 1, Detection Results, Equipment and Techniques, p. 57-90.

Naval Research Laboratory
Technical Library
Research Reports Section

DATE: July 1, 2002

FROM: Mary Templeman, Code 5227

TO: **Code 5300 Paul Hughes**

CC: Tina Smallwood, Code 1221.1 8/21/02

SUBJ: Review of NRL Reports

Dear Sir/Madam:

Please review NRL Reports ~~7583~~, ~~7631~~, 7752, 7765, and MR-3079 for:

- ☑ Possible Distribution Statement
- ☐ Possible Change in Classification

Thank you,

Mary Templeman

Mary Templeman
(202)767-3425
maryt@library.nrl.navy.mil

The subject report can be:

- ☑ Changed to Distribution A (Unlimited) for Reports 3079, 7765, AND 7752
- ☐ Changed to Classification _____
- ☑ Other: Reports 7583 AND 7631 should retain there limited distribution statements

Paul K. Hughes IV 8/21/2002

Signature Date

-- 1 OF 1
-- 1 - AD NUMBER: 531281
-- 2 - FIELDS AND GROUPS: 15/4, 17/9
-- 5 - CORPORATE AUTHOR: NAVAL RESEARCH LAB WASHINGTON D C
-- 6 - UNCLASSIFIED TITLE: PROBABILITY OF DETECTING SHIPS WITH AN OTH
-- RADAR SYSTEM.
-- 9 - DESCRIPTIVE NOTE: INTERIM REPT.,
--10 - PERSONAL AUTHORS: WILSON,JON DAVID ;
--11 - REPORT DATE: 10 JUL 1974
--12 - PAGINATION: 48P MEDIA COST: $ 7.00 PRICE CODE: AA
--14 - REPORT NUMBER: NRL-7765
--16 - PROJECT NUMBER: NRL-R02-46A, WF12-111
--17 - TASK NUMBER: WF12-111-704
--20 - REPORT CLASSIFICATION: UNCLASSIFIED
--22 - LIMITATIONS (ALPHA): DISTRIBUTION LIMITED TO U.S. GOV'T.
-- AGENCIES ONLY; TEST AND EVALUATION; JUL 74. OTHER REQUESTS FOR
-- THIS DOCUMENT MUST BE REFERRED TO DIRECTOR, NAVAL RESEARCH LAB.,
-- WASHINGTON, D. C. 20375.
--23 - DESCRIPTORS: (*OVER THE HORIZON DETECTION, *RADAR), (*SHIPS,
-- OVER THE HORIZON DETECTION), PROBABILITY, OCEAN SURVEILLANCE, SEA
-- CLUTTER, IONOSPHERIC PROPAGATION, COMPUTER PROGRAMS, COST
-- EFFECTIVENESS, RADAR SIGNALS, PROPAGATION, RADAR EQUIPMENT,
-- SPACEBORNE, AIRBORNE, GROUND STATIONS, TARGET ACQUISITION,

-
-- DETECTION
--24 - DESCRIPTOR CLASSIFICATION: UNCLASSIFIED
--25 - IDENTIFIERS: RADARC COMPUTER PROGRAMS
--26 - IDENTIFIER CLASSIFICATION: UNCLASSIFIED